The interplay between eosinophils and macrophages in malignant pleural mesothelioma immunotherapy

Auteur : Dagneaux, Emeline
Promoteur(s) : Willems, Luc; Halkin, Louise
Faculté : Gembloux Agro-Bio Tech (GxABT)
Diplôme : Master en bioingénieur : chimie et bioindustries, à finalité spécialisée
Année académique : 2023-2024
URI/URL : http://hdl.handle.net/2268.2/19710

LIÈGE université
Gembloux
Agro-Bio Tech

THE INTERPLAY BETWEEN EOSINOPHILS AND MACROPHAGES IN MALIGNANT PLEURAL MESOTHELIOMA IMMUNOTHERAPY

EMELINE DAGNEAUX

TRAVAIL DE FIN D'ÉTUDES PRÉSENTÉ EN VUE DE L'OBTENTION DU DIPLÔME DE MASTER BIOINGÉNIEUR EN CHIMIE ET BIO-INDUSTRIES

ANNÉE ACADÉMIQUE 2023-2024

PROMOTEUR: WILLEMS LUC

CO-PROMOTRICE : HALKIN LOUISE

[1] L'autorité académique est représentée par le promoteur, membre du personnel enseignant de GxABT (Luc Willems)

HOME INSTITUTION

This master thesis has been realised within the cellular and molecular epigenetics (CME) laboratory of the GIGA institution, a multidisciplinary biomedical research centre of the University of Liege, closely linked to the Sart-Tilman “Centre Hospitalier Universitaire” (CHU). Created in 2003, the GIGA is composed of nine technological platforms, nine research units and more than 600 scientists from 45 different countries from five faculties (Gembloux Agro-Bio Tech, Sciences, Applied Sciences, Medicine and Veterinary medicine). Among the research units, the GIGA-Cancer study the genesis, development, proliferation and resistance of cancers to conceive adapted treatments for each patient. The CME accounts for one of the seven laboratories of GIGA-Cancer and employs three post-doctorates, eight PhD students and one technician.

ACKNOWLEDGEMENTS

Pour commencer, je tiens à remercier toutes les personnes qui ont contribué, de près ou de loin, à la réalisation de ce mémoire.

Dans un premier temps, je voudrais remercier le Professeur Luc Willems de m'avoir permis de réaliser ce mémoire au sein de son équipe. Merci également pour les nombreux échanges et les conseils avisés.

Ensuite, je tiens à remercier Louise Halkin pour son encadrement, ses précieux conseils, sa bienveillance et toutes les connaissances transmisses au cours de ces 6 mois de laboratoires. Merci pour les nombreuses relectures et la confiance que tu m'as accordée.

Je souhaite également remercier l'équipe du laboratoire EPI : Mégane Willems, Alexis Fontaine, Roxane Terres, Aurélie Beauvois, Léa Vilanova Mana, Xavier Saintmard, Ning Yang, Jean-Rock Jacques, Thomas Jouant, Thomas Joris et Malik Hamaïdia. Merci pour le soutien apporté, la bonne ambiance quotidienne et les happy hours de chocolats chauds. Je tiens à remercier tout particulièrement Mégane pour sa disponibilité et ses relectures attentives de la partie éosinophile, ainsi que Malik pour son encadrement et ses conseils dans l'apprentissage de la culture de macrophages primaires.

J'aimerais également remercier Colleen et Dina pour leur soutien moral sans failles. Merci pour votre écoute et votre présence dans les bons et les mauvais moments. Je n'y serai jamais arrivée sans vous. Merci également à la team des chimistes pour leur bonne humeur durant les nuits de rédaction et leur aide face aux cours et particulièrement à Sarah, la meilleure partenaire de belottes. Je souhaite également remercier les habitants du Néon's pour ces 3 années de colocation remplies de soupers kot et de victoire à l'Interkot et à toutes ces personnes exceptionnelles que j'ai pu rencontrer dans ces vieux murs de Gembloux.

Last but least, je tiens également à remercier mes parents de m'avoir soutenue pendant ces 5 longues années d'études et ma sœur et mon frère pour tous les fous rires et les moments partagés depuis notre enfance, ainsi que toute ma famille, en particulier mes grands-parents, d'avoir toujours cru en moi, plus que ce que je n'aurais jamais pu faire.

ABSTRACT

Malignant pleural mesothelioma (MPM) is a rare and aggressive cancer arising in the mesothelial cells of the pleura, mostly after asbestos exposure. Patients overall survival remains poor and treatments are only palliative. In 2020, the Food and Drug Administration (FDA) approved an immunotherapeutic treatment combining two immune checkpoint inhibitor drugs, nivolumab and ipilimumab, respectively anti-programmed cell death (PD)-1 and anti-cytotoxic T-lymphocyte-associated protein (CTLA)-4. Macrophages are versatile immune cells, able to polarise into two contrary phenotypes (M1 and M2), according to environmental stimuli. Both phenotypes can exert opposite functions on tumour growth and inflammation regulation. In MPM, tumour-associated macrophage (TAM) infiltration in the tumour microenvironment (TME) is correlated with poorer prognostic. Meanwhile, a high peripherical blood eosinophil count has been related to inferior survival in MPM patients. Therefore, this master thesis aims to study the impact of human eosinophil supernatant on primary macrophage cytotoxicity towards MPM cells in an immunotherapeutic context. Results demonstrate that eosinophils downregulate PD-1 and PD-ligand (PD-L)-1 expression in polarised macrophages.

RÉSUMÉ

Le Mésothéliome Pleural Malin (MPM) est un cancer rare et agressif qui survient dans les cellules mésothéliales de la plèvre, principalement après une exposition à l'amiante. La survie globale des patients demeure faible et les traitements ne sont donnés qu'à titre palliatif. En 2020, l'Administration de l'Alimentation et des Médicaments a approuvé le traitement immunothérapeutique qui combine deux médicaments inhibiteurs de points de contrôle immunitaire, nivolumab et ipilimumab, respectivement anti-mort cellulaire programmée (PD)-1 et anti-protéine associée aux lymphocytes T cytotoxiques (CTLA)-4. Les macrophages sont des cellules immunitaires polyvalentes, capables de se polariser en deux phénotypes contraires (M1 et M2), en fonction des stimuli environnementaux. Ces deux phénotypes peuvent exercer des fonctions opposées dans la croissance tumorale et la régulation de l'inflammation. Dans le MPM, l'infiltration des macrophages associés à la tumeur dans le microenvironnement tumoral corrèle avec un prognostique plus faible. D'autre part, un taux d'éosinophiles élevé dans le sang périphérique est lié à une survie inférieure chez les patients atteints de MPM. Par conséquent, ce mémoire vise à étudier l'impact du surnageant d'éosinophiles humains sur la cytotoxicité des macrophages primaires envers les cellules de MPM dans un contexte d'immunothérapie. Les résultats démontrent que les éosinophiles régulent à la baisse l'expression de PD-1 et de PD-ligand (PD-L)-1 chez les macrophages polarisés.

LIST OF ABBREVIATIONS

8-OHdG	8-hydroxydeoxyguanosine
AnPC	Antigen-presenting cells
APC	Allophycocyanin
ARG	Arginase
c/EBP	CCAAT/enhancer-binding protein
CCL	Chemokine ligand
CCR	C-C chemokine receptor
CD	Cluster of differentiation
CFSE	Carboxyfluorescein succinumidyl ester
CLC	Charcot-Lyden crystals
CME	Cellular and molecular epigenetics
CMP	Common myeloid progenitor
CTLA	Cytotoxic T-lymphocytes-associated protein
DAMP	Damage-associated molecular pattern
DC	Dendritic cells
DMEM	Dulbecco's Modified Eagle Medium
dNTP	Deoxyribonucleotides
ECM	Extracellular matrix
ECP	Eosinophil cationic protein
EDN	Eosinophil-derived neurotoxin
EDTA	Ethylenediamine tetraacetic acid
EGF	Endothelial growth factor
ELISA	Enzyme-linked immunosorbent assay
EMP	Erythro-myeloid progenitor
EoP	Eosinophil progenitors
EPO	Eosinophil peroxidase
FBS	Fœtal bovine serum
Fc	Fragment crystallisable
FDA	Food and Drug Administration
FITC	Fluorescein isothiocyanate
FSC	Forward scatter
GM-CSF	Granulocyte-macrophage colony-stimulating factor
GMP	Granulocyte and macrophage progenitor
GTP	Guanosine triphosphate
HE SN	Human eosinophil supernatant
HLA	Human leucocyte antigen
HMGB	High mobility group box
HSC	Haematopoietic stem cells
IC	Immune complexes
IFN	Interferon
IL	Interleukin
LPS	Lipopolysaccharides
MBP	Major basic protein

MCP	Monocyte chemoattractant protein
M-CSF	Macrophage colony-stimulating factor
MDM	Monocyte-derived macrophage
MDP	Monocytes and DC progenitor
MDSC	Myeloid-derived suppressor cells
MEM NEAA	Minimum essential medium non-essential amino acids
MHC	Major histocompatibility complex
MPM	Malignant pleural mesothelioma
NET	Neutrophil extracellular trap
NK	Natural killer
NO	Nitric oxide
OS	Overall survival
PBMC	Peripherical blood mononuclear cells
PBS	Phosphate-buffered saline
PD-1	Programmed cell death protein-1
PD-L1	Programmed cell death protein ligand 1
PenStrep	Penicillin and Streptomycin
PI	Propidium iodide
PMN	Polymorphonuclear
PRR	Pattern-recognition receptors
RAGE	Receptor for advanced glycation end-products
RBC	Red blood cells
rh	recombinant human
rMFI	relative median fluorescence intensity
RNI	Reactive nitrogen intermediates
ROI	Reactive oxygen intermediates
ROS	Reactive oxygen species
RPMI	Roswell Park Memorial Institute
SD	Standard deviation
SSC	Side scatter
TAM	Tumour-associated macrophage
TCR	T-cell receptor
TGF	Transforming growth factor
Th	T-lymphocyte helper
TIL	Tumour-infiltrating lymphocyte
TLR	Toll-like receptors
TME	Tumour microenvironement
TNF	Tumour necrosis factor
Tregs	Regulatory T-cells
VEGF	Vascular endothelial growth factor

LIST OF FIGURES

LIST OF TABLES

TABLE OF CONTENTS

PART I

INTRODUCTION

I. INTRODUCTION

1. Malignant Pleural Mesothelioma

1.1. General information

Malignant pleural mesothelioma (MPM) is a rare and aggressive cancer arising in the mesothelial cells of the pleura, a serous membrane surrounding the lungs. Among other forms of mesothelioma occurring in the peritoneum, pericardium and tunica vaginalis, MPM represents 80%[1]. The prognosis remains poor, with an overall survival (OS) between 7 and 17 months after diagnosis[2]. In 70% of cases, mesothelioma is caused by asbestos and develops commonly 30 to 40 years after exposure[2]. However, the incidence of exposed workers developing MPM is weak and usually occurs within the same families, highlighting a potential genetic predisposition[3]. Average symptoms include coughing, fatigue, chest wall pain, breathlessness and weight loss, but pleurisy and cachexia can also occur in late-stage MPM[1,2].

1.2. Asbestos

The term “asbestos” includes six natural fibrous minerals formed during rock metamorphism[1,4]. Asbestos fibre structure is filamentous and has a length-to-width ratio greater than 3:1, endowing numerous properties, such as acoustic insulation, high thermic resistance and incombustibility[1,4]. The uses of asbestos are numerous and encompass many fields, from building and ship construction to the textile industry. In total, 3000 to 4000 products have been created with asbestos since its discovery in Canada. Chrysolite, the most commercialised form, accounts for 90 to 95% of the production[4]. For years, the use of asbestos has been correlated with the development of some diseases, namely asbestosis and different forms of mesothelioma, mostly in men as, historically, mines and construction are two masculine sectors[5]. Therefore, up to 50 countries have banned its extraction and use, including Belgium in 2001. Still, asbestos remains highly dormant in our buildings and regularly makes headlines because removal stays exorbitantly expensive[4,6]. Anyhow, asbestos is still highly employed in underdeveloped countries in Africa, Asia and South America due to its cheapness[4,5].

1.3. Histology

In MPM, three different histological subtypes can be identified depending on the features of mesothelial cells. Epithelioid MPM is the most common one (71%), followed by biphasic (17%) and sarcomatoid (12%)[7], even though percentages may vary from one study to another[2,8–12]. The epithelioid form is composed of epithelial cells that are flat, polygon-,

round- or cube-shaped and organised in papillary formations, sheets or tubules. The epithelioid subtype can be subdivided into several subtypes, all characterised by a low mitosis frequency. Meanwhile, sarcomatoid MPM is constitute with fusiform cells disposed randomly or in fascicles. The biphasic subtype involves both epithelioid and sarcomatoid forms, with a prevalence lower than 90%[9,10].

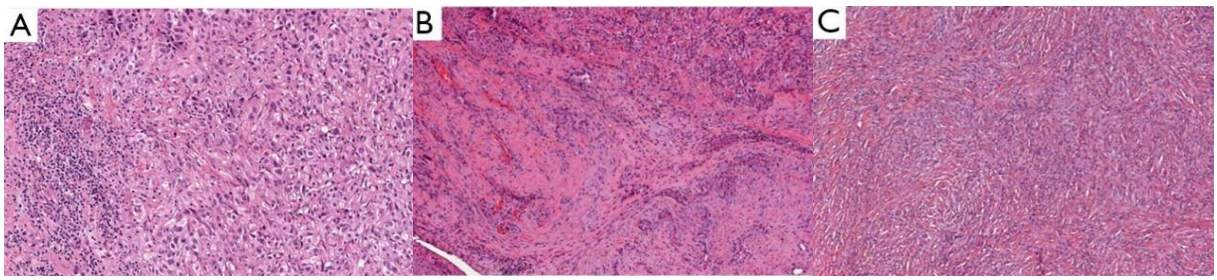

Figure 1 – **Histologic images of the three MPM subtypes**. (**A**) Epithelioid. (**B**) Biphasic. (**C**) Sarcomatoid. Adapted from L. Brcic and I. Kern (2020)[11].

The sarcomatoid subtype is known to be the most aggressive form, with an OS of 8 months, while the epithelioid subtype is the less aggressive, with an OS of 20 months. Concerning the biphasic subtype, OS highly depends on the predominant form, with a median survival of around 13 months[7].

1.4. Oncogenesis

How asbestos fibres reach the pleura is still not fully understood, but it has been established that thicker and longer fibres penetrate deeper[12]. Asbestos induces mesothelioma through chronic inflammation, causing oxidative stress, *i.e.*, a disproportion between the production of free oxidant molecules and the capacity to promptly neutralise them[13]. Several complementary processes, all linked to the presence of asbestos in the pleura, are involved in the production of highly reactive Reactive Oxygen Species (ROS), resulting from the incomplete reduction of dioxygen[13].

Firstly, iron combined with asbestos fibres enhances the production of HO· radicals coming from H_2O_2, via the oxidation of Fe^{2+} into Fe^{3+}, known as the Fenton reaction (**Figure 2A**)[14]. Recent studies have also shown that resistance to ferroptosis, an iron-dependent non-apoptotic cell death, may be linked to mesothelioma development[15]. Secondly, mesothelial cells in contact with asbestos fibres secrete pro-inflammatory cytokines and growth factors, inducing an inflammatory storm and immune cells recruitment. Soluble mediators overactivate them and induce ROS production (**Figure 2B**)[12,13]. Afterwards, the longest asbestos fibres are too massive to be phagocytosed by macrophages. Those "frustrated" macrophages discharge ROS (**Figure 2C**) and undergo programmed cell necrosis, releasing high mobility group box 1 (HMGB1), a damage-associated molecular pattern (DAMP) able to activate the inflammasome[13,16].

ROS overabundance disrupts numerous cell processes involving genetic and epigenetic transformation, including cell growth, genomic stability, resistance to apoptosis and metastatization[13,14]. In MPM, DNA bases can be oxidised by ROS which can lead, if inadequately repaired, to incompatible pairing between bases and further cancerous mutations[14]. For instance, 8-hydroxydeoxyguanosine (8-OHdG) is one of the predominant ones, involving a transversion from G to T, and can be highly mutagenic[17].

Ultimately, the potential carcinogenicity of mineral fibres is ruled by their dimensions, durability, dose and physical properties; *e.g.*, longer fibres are correlated with an increase in "frustrated phagocytosis"[16]. Likewise, other factors, including genetic, environmental and intracellular antioxidants may also contribute to oncogenesis[16,17].

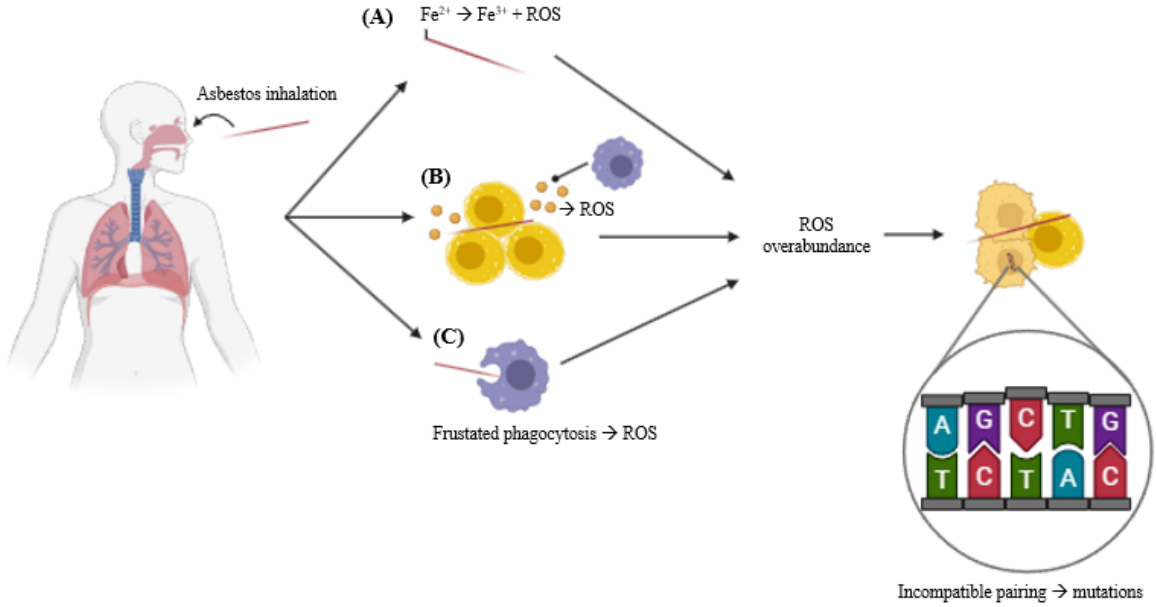

Figure 2 – **Hypothetical mechanisms of MPM oncogenesis after asbestos exposure**. (**A**) Iron ions linked to asbestos fibres react into Fe^{3+}, creating ROS in the process. (**B**) Asbestos induces MPM express cytokines that attract macrophages and enhance ROS production. (**C**) Frustrated phagocytosis by macrophages releases ROS. Ultimately, the ROS overabundance leads to DNA damage and mismatched pairing. The figure was created on the BioRender.com website.
Abbreviations : MPM, malignant pleural mesothelioma; ROS, reactive oxygen species.

1.5. Tumour microenvironment

Over the past years, the importance of the tumour microenvironment (TME) has been revealed with constantly increasing research numbers on its impact on numerous cancer[18]. The TME is built up with a highly heterogeneous mixing of endothelial, stromal and immune cells, all multiply and complexly interacting with each other[8,14,18]. The TME tendency to be immunosuppressive may explain the persistence of MPM and associated-OS[18,19]. Its composition is highly variable, depending primarily on histologic types and patients, and may be essential for correct prognostic and convenient treatments[8,20].

Among immune cells present in the TME, tumour-associated macrophages (TAMs) are the most predominant (cf. 2.5. TAMs), followed by tumour-infiltrating lymphocytes (TILs), which constitute between 20 and 42%[19]. Originating from the bone marrow, T- cells transit in the vascular system to reach the thymus gland, where they mature into different species of effector T-cells, identified based on expressed membrane receptors[12,18]. The most abundant[14] are clusters of differentiation 8^+ ($CD8^+$) cells, specialised in apoptosis of dangerous cells via the release of cytotoxic cytokines and molecules[12]. Prevailing in sarcomatoid and biphasic subtypes[12], $CD8^+$ T-cells can also recognise antigens and bind to the major histocompatibility complex-I (MHC-I), using their T-cell receptor (TCR)[18]. Besides, $CD4^+$ T-lymphocyte helper (Th), dominant in the circulating blood of epithelioid patients[12], can generate an antitumoral response through antigen-presenting cells (AnPCs) and produce interferon gamma (IFN-γ) and interleukin-2 (IL-2). Both are known to stimulate $CD8^+$ T-cells and Natural Killers (NKs), enhancing their cytotoxicity[12,19]. Lastly, $CD4^+$/$FoxP3^+$ T-cells[19], or regulatory T-cells (Tregs), downregulate $CD4^+$ and $CD8^+$ T-cells, encouraging immunosuppresivity[12]. Consequently, Tregs are associated with higher risks of death and MPM relapse after treatment[12,19]. In cases of persistent stimulation of TCRs and co-inhibitory signals due to the immunosuppressive TME, TILs can gradually forfeit their effector functions and become "exhausted". Expression of co-inhibitory receptors, like programmed cell death protein-1 (PD-1) and cytotoxic T-lymphocyte-associated protein 4 (CTLA-4), is also progressively upregulated, preventing activation and proliferation of T-cells in tumour[14]. However, no relation between exhaustion markers and OS has been established[21].

The immune TME is also built up of B lymphocytes, NKs, dendritic cells (DCs) and myeloid-derived suppressor cells in slightest amounts. B-cells are enlisted in TME by TAMs stimulatory signals and involved in higher OS[18]. They have multiple roles, from activating T-cells as an AnPC to differentiating into antibody-secreting plasma cells and supplying humoral immunity[18,19]. Anyhow, in murine models, B-cell infiltration seems to boost chronic inflammation and, thereby, tumour development[18], contrasting with current knowledge on human patients. Besides, NK's initial function is detecting and eradicating cells expressing low or no amounts of human-leukocyte antigen. In TME, their cytotoxicity depends on the kind of receptor expressed on their surface, either an activating or a suppressive one[12]. Another type of AnPC present in the TME are DCs, derived from the same precursors as monocytes (cf. 2.1. Origin)[12]. DCs play a role in regulating immune response by activating naïve T-cells and regulating their response, but also contribute to instituting an immunosuppressive TME[12,19]. Furthermore, MPM patients present lower concentrations of circulating DCs[12]. However, doubts about the actual difference between DCs and macrophages remain sharp and highly debated among specialists[22,23].

Lastly, MPM cells themselves are able to actively escape the immune system by inhibiting immune checkpoints. This process is enabled through Darwinian selection of the most-adapted malignant cells for the host TME[14,18].

1.6. Treatments

1.6.1. Surgery

In MPM, surgical use should be combined with other sorts of treatments and considered palliative. Moreover, complete resection is impossible and not all patients can undergo surgery, depending mainly on their age and disease stage[2,24]. Two options coexist: either complete extraction of the tumour, the pleura and sometimes the diaphragm or extrapleural resection of the diaphragm, tumour, lung tissue and parietal pleura[2,25]. The choice between those two options depends on the subtype and progression stage[25]. However, the efficiency of this treatment is still debated in the scientific community, since postoperative morbidity and mortality rates remain critical[26]. Likewise, no study has undoubtedly demonstrated an improvement in OS for surgery patients[2,24].

1.6.2. Radiotherapy

Radiotherapy is deemed in palliative settings to reduce chest wall pain in a trimodal procedure with surgery and chemotherapy[2,24,25]. Nevertheless, no study proves enhanced OS in radiotherapy cases[24] and the treatment contains side effects ranging from nausea and exhaustion to skin irritation[2].

1.6.3. Chemotherapy

Chemotherapy treatment is based on the combination of cisplatin and pemetrexed and was the first in 2004, to receive Food and Drug Administration (FDA) approval for MPM treatment. Cisplatin, constituted with one platinum and two chlorine atoms, endures an aquation, or non-enzymatic substitution of a ligand by a water molecule, and generates inter- and intrastrand DNA adducts, which block DNA replication in the S phase. Meanwhile, pemetrexed is an antifolate complex, entering the cell through the reduced folate carrier. Once in the cytoplasm, it becomes polyglutamated and inhibits the synthesis of new deoxyribonucleotides (dNTPs), leading to a reduction in cellular replication[2,14].

Despite the fact that chemotherapy increases the OS by 6.1 months, numerous side effects, including diarrhoea, myelosuppression, nausea, tiredness, vomiting, dehydration and, in the worst case, neutropenia and leukopenia, make it unsuitable for several patients[2,8,25]. Additionally, chemoresistant cells are advantaged and can proliferate into an MPM unresponsive to cisplatin and pemetrexed toxicity[14].

1.6.4. Immunotherapy

In 2020, the immunotherapeutic treatment combining two immune checkpoint inhibitor drugs, nivolumab and ipilimumab, respectively anti-PD-1 and anti-CTLA-4, was approved by the FDA ensuing the Checkmate 743 trial[25,27]. The survey, conducted on 605 randomised patients,

has demonstrated a significantly enhanced median OS for immunotherapy towards chemotherapy (18.1 vs 14.1 months) and a 2-year OS rate of 40.8% (versus 27.0%), for a similar response rate (40 versus 43%)[25,28]. Despite all those benefits, immunotherapy, as chemotherapy, shows numerous side effects, *i.e.*, healthy organs inflammation, exhaustion and diarrhoea[27].

PD-1 is displayed by lymphocytes[19], macrophages and DCs[29] and its ligand, PD-L1, is highly expressed by cancerous cells[19,30], especially from non-epithelioid histology[19]. Interaction between MPM PD-L1 and T-lymphocyte PD-1 prohibits their activation and proliferation[19], while association with macrophages PD-1 reduces their cytotoxic and phagocytic properties[30]. Hence, nivolumab, by binding to PD-1, restores both T-cell and macrophage immune functions[19,29]. Furthermore, CTLA-4, a glycoprotein present on T-cells surface, binds to CD80/CD86, displayed by AnPCs and restrains their interaction with CD28 receptors of T-lymphocytes, required for T-cell activation[12,18].

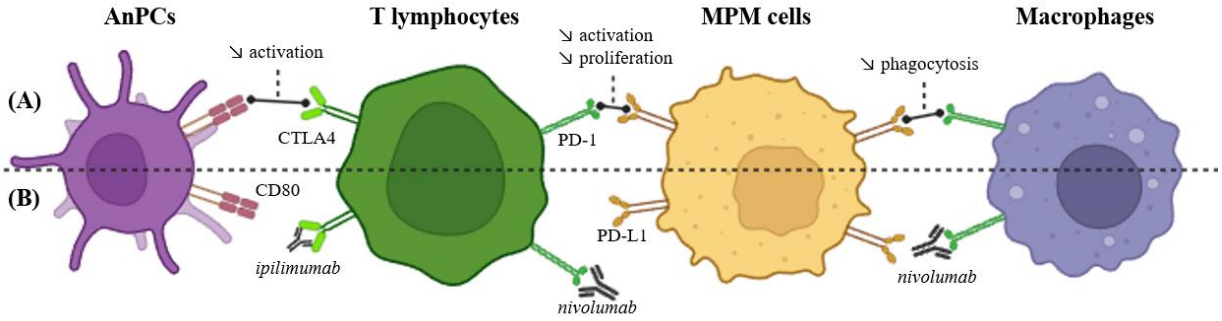

Figure 3 – **Effect of immunotherapy on immune cells**. (**A**) Mechanisms of immune escape of MPM cells. (**B**) Mode of action of ipilimumab (anti-CTLA-4) and nivolumab (anti-PD-1). The figure was created on the BioRender.com website.
Abbreviations : AnPC, antigen-presenting cells; MPM, malignant pleural mesothelioma; CTLA, cytotoxic T-lymphocyte-associated protein; CD, cluster of differentiation; PD-1, programmed death cell-1; PD-L1, PD-ligand 1.

New treatment approaches using pulsed-DCs are being assessed to reinvigorate T-cells from exhaustion. Indeed, T-cell numbers tend to fall after chemotherapy and DCs represent only a small percentage of MPM-infiltrated cells; hence, pulsed-DCs treatment after chemotherapy may restore T-cell functions and has shown interesting results on restricted clinical tests with no major side-effects[12,18]. Alternatively, adding bevacizumab to the cisplatin-pemetrexed combination has been attempted and may expand OS by 2.7 months[8,18]. This monoclonal antibody targeting vascular endothelial growth factor (VEGF) might probably adjust tumoral microvasculature[8]. Nonetheless, grade 3 side effects, namely hypertension and thrombosis, seem to increase in patients cured with bevacizumab[25]. Hence, these treatments remain actively discussed among the scientific community and have not received FDA approval yet[24,25].

2. Macrophages

Macrophages are mononuclear cells of the innate immune system[31]. They are highly versatile and epigenetically and phenotypically heterogeneous, depending on their origin, tissue of residence and microenvironmental signals[22,32,33]. Although macrophages can have various names depending on tissue location, *e.g.*, osteoclasts in bones or alveolar macrophages in lungs, their roles remain roughly the same, including immune response against pathogens, maintenance of homoeostasis and monitoring of tissue changes[22].

2.1. Origin

Macrophages arise from two different lineages, even though no morphological distinction can be established depending on the origin[22]. During pregnancy, embryonic precursors spread into tissues and differentiate into the majority of tissue-resident macrophages, self-renewing themselves through adulthood[22,33]. In homeostatic conditions, prenatal macrophages generally suffice to maintain the pool of tissue-resident macrophages, as in monocytopenia patients[22]. Meanwhile, in inflammatory conditions, monocyte-derived macrophages (MDMs) emerge from blood-circulating monocytes, which are yielded in the bone marrow, and represent the majority of TAMs[22,33].

2.1.1. Embryonic origin

Embryonic macrophages seed foetal tissue in two distinct waves[22]. Firstly, during early gestation, erythro-myeloid progenitors (EMP) generate the first supply of embryonic macrophages[22,33]. This phase is called primitive haematopoiesis. Around half-pregnancy, EMPs wreak foetal liver and fulfil the embryonic vasculature with circulating monocytes[22,34].

2.1.2. Monocyte-derived macrophages

After birth, haematopoietic stem cells (HSCs) from the foetal liver populate the bone marrow using blood vessels and engender monocytes, following a succession of intermediate progenitors (**Figure 4**)[22,34]. Differentiation of monocytes into macrophages is largely mediated by macrophage colony-stimulating factor (M-CSF) produced by stromal cells and tissue environment[22,32]. *In situ*, depending on the tissue, other growth factors can contribute, such as granulocyte-M-CSF (GM-CSF) for alveolar macrophages[32]. Monocytes are irregular-shaped cells with a high cytoplasm-to-nucleus ratio, accounting for roughly 5-10% of human leucocytes[22,35]. Once differentiated, monocytes enter the blood flow and circulate for a couple of days[22,35]. In cases of infection or chronic inflammation, circulating monocytes are recruited in tissue as MDMs to reinforce macrophage stock. Under homeostatic conditions, monocytes can also complete tissue-resident macrophage pools, especially in the gut and colon[32,33].

Two monocyte subpopulations can be discerned depending on CD14 and CD16 surface markers expression[22,32]. 90% express no CD16 but high CD14 and are named classical or

$CD14^{++}CD16^{-}$ monocytes [22,32]. With $CD14^{++}CD16^{+}$, they embody inflammatory monocytes engaged on inflammatory sites and discharging pro-inflammatory cytokines. Aside, $CD14^{dim}CD16^{+}$ is termed patrolling monocytes through their faculties to scour the vasculature and assimilate cellular debris[32]. Despite the long-lasting thought that monocytes are merely dormant progenitors of macrophages, recent studies have shown that they could actually be innate effector cells, contributing to inflammatory, pathogen eradication, antigen presentation, homoeostasis and phagocytosis. However, one question is still pending about the reason for having two distinct monocyte subsets. Scientists are currently debating whether it stands for different maturation stages achieved by classical monocytes or end-stages of separate pathways[22].

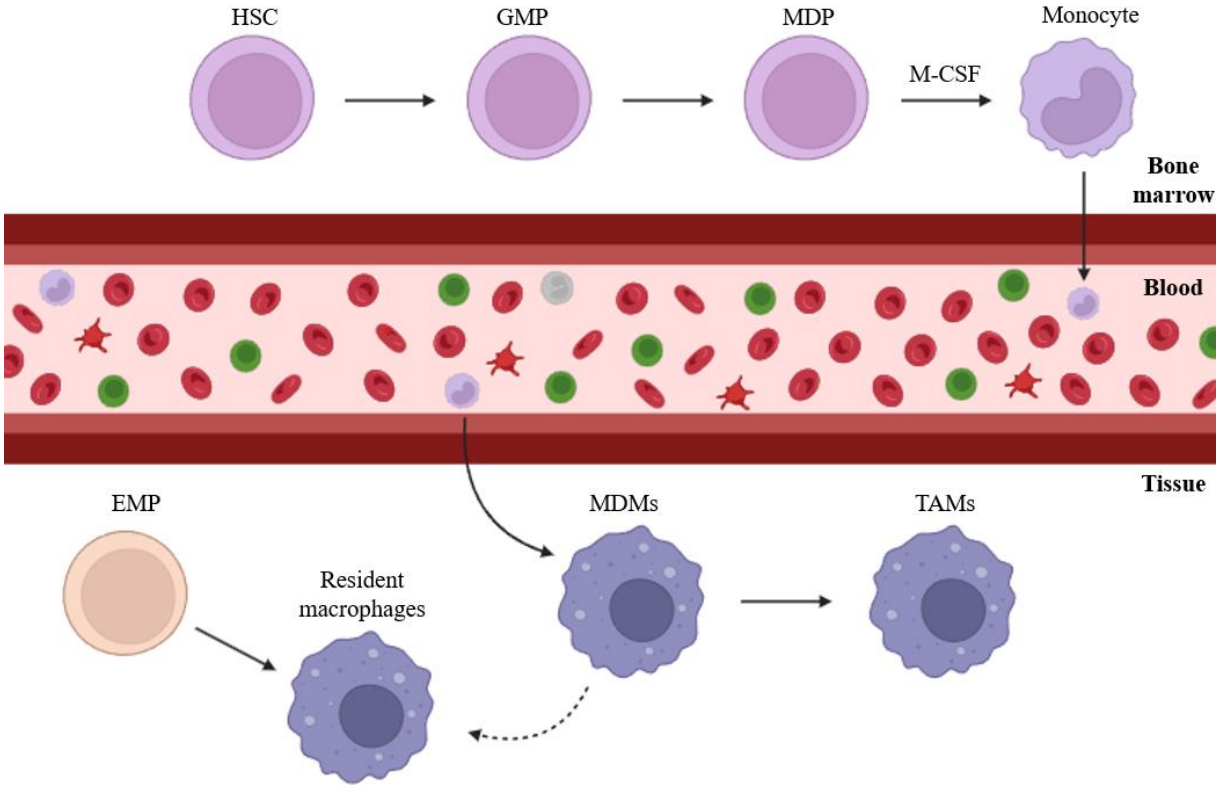

Figure 4 – **Macrophages haematopoiesis**. HSC from the bone marrow evolves into GMP, which further turns into MDP. In presence of M-CSF, MDP differentiates into monocytes, that enter the blood circulation. If needed in tissues, monocytes infiltrate it to become MDM and, in case of oncogenesis, TAMs. Besides, tissue-resident macrophages arise from EMP during embryogenesis. In some tissues, MDMs can complete the existing pool of macrophages. The figure was created on the BioRender.com website.

Abbreviations : HSC, haematopoietic stem cells; GMP, granulocyte and macrophage progenitors; MDP, monocytes and DC progenitors; DC, dendritic cells; M-CSF, macrophage colony-stimulating factor; EMP, erythro-myeloid progenitors; MDMs, monocytes-derived macrophages; TAMs, tumour-associated macrophages.

2.2. Activation pathways

MDMs have two activation pathways depending on molecules in their microenvironment and display a huge amplitude of phenotypes, chemokine production and associated functions[22,30,32]. In 2000, Mills and al. introduced the M1/M2 models standing for the Th1/Th2 polarisation[36]. Nevertheless, even though $CD4^+$ T-cells may direct macrophage polarisation during inflammatory responses[22,36], recent research has shown that macrophage activation is not mandatorily coupled with T-cell functions, which only amplify it via IL-4 and IFN-γ production[22]. Moreover, the M1/M2 paradigm appears incomplete in relation to new findings on macrophage plasticity and pleiotropy, highlighting a continuum having the M1- and M2-phenotypes as end-points[22,30,32,33]. *De facto*, macrophage phenotype is driven multidimensionally by a complex interaction of numerous stimuli[32]. Indeed, *in vivo*, macrophages can exhibit a phenotype with both M1- and M2-features[32].

The classical activation pathway yields pro-inflammatory and antitumoral M1-macrophages, an $IL\text{-}12^{high}IL\text{-}23^{high}IL10^{low}$ phenotype specialised in pathogens and cancer cell removal[22,32,33]. This pathway is powered by inflammatory molecules, notably IFN-γ and tumour necrosis factor alpha (TNF-α), and microorganism-related molecules, particularly lipopolysaccharides (LPS) produced by Gram-negative bacteria[22,32,33]. M1-macrophages express MHC-II molecules and pro-inflammatory cytokines, such as IL-1β, IL-6, IL-12 and TNF, as well as reactive nitrogen and oxygen intermediates (RNI and ROI), which display tumoricidal features and promote Th1 effector responses[22,32,37]. In addition, the M1-phenotype overexpresses CD16/32, CD80 and CD86 surface markers[37] and has an arginine metabolism turned for citrulline and nitric oxide (NO) output, key cytotoxic molecules for their inhibitory effect on cell spreading and antimicrobial action[22].

Meanwhile, the alternative activation pathway provides anti-inflammatory and pro-tumoral M2-macrophages, a $IL\text{-}12^{low}$ $IL\text{-}23^{low}$ $IL\text{-}10^{high}$ transforming growth factor (TGF)-β^{high} phenotype, that take part in damaged-tissue remodelling, homoeostasis, nematode eradication, immunoregulation, angiogenesis and phagocytosis[22,32,33]. The M2-pathway is switched on by anti-inflammatory cytokines (IL-4 and IL-13[32,37]), and converts arginine metabolic processes into ornithine and polyamine production, promoting tissue repair and cell proliferation[22,32]. The M2-phenotype highly expresses IL-10, CD163, CD204, CD206, arginase (ARG)-1 and human-leukocyte antigen (HLA)-DR[33,35,37] and is usually the "as default" phenotype for tissue-resident macrophages[22]. It can have several subphenotypes according to the pathway-pioneer stimulus[22].

During inflammatory scenarios, two waves of monocyte polarisation generally occur. Firstly, MDMs display a M1-phenotype to combat troubling cells and commonly perish under their own NO production. The second wave aims to reconstruct and repopulate tissue with M2-MDMs[22]. Furthermore, research has shown that tissue-resident M2-macrophages can switch to the M1-phenotype as response to the pro-inflammatory microenvironment[22,32], leading to questionings about whether the M2-phenotype is an intermediate phenotype of the end-stage

killer M1-phenotype or both are separate subpopulations with their respective roles[22]. An answer may reside in the fact that reverse shift generally does not occur or only in very specific conditions, such as sepsis, *Listeria* infection or skeletal muscle injury[22,32].

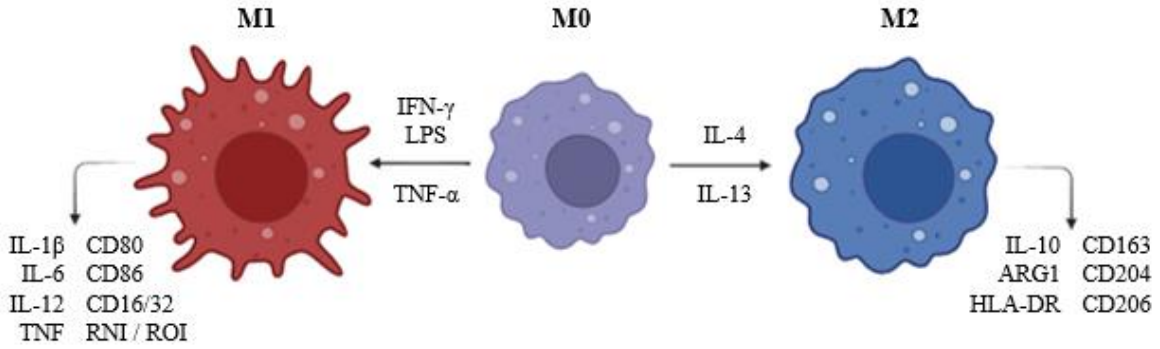

Figure 5 – **M1/M2 macrophage polarisation model**. Depending on environmental stimuli, macrophages can produce dissimilar cytokines and express different receptors. The figure was created on the BioRender.com website.
Abbreviations : IFN, interferon; LPS, lipopolysaccharides; TNF, tumour necrosis factor; IL, interleukin; CD, cluster of differentiation; RNI, reactive nitrogen intermediate; ROI, reactive oxygen intermediate; HLA, human-leukocyte antigen.

2.3. Functions

Even though macrophages can have side-roles on angiogenesis, immunoregulation, immune memory and tissue development, only the three main functions, namely phagocytosis, antigen presentation and cytokine production, will be discussed below[22,32,35,38].

2.3.1. Phagocytosis

Phagocytosis characterises the process of eukaryotic cells recognising and engulfing a particle with a diameter larger than 0.5µm and digesting it by acidification and proteolysis[32,39–41]. Tissue-macrophages are highly phagocytic to clear apoptotic cells and eliminate pathogens[22,39].

Phagocytosis happens in three main steps[39,40]. Firstly, macrophages recognise the future phagosome through pattern-recognition receptors (PRRs). Different types of receptors are known based on the particle's category[39,40]. For instance, Fc (Fragment crystallisable) receptor-mediated phagocytosis occurs in the presence of IgG-binding pathogens and triggers inflammation via pro-inflammatory cytokines and ROS release, while mannose receptors (CD206) and apoptotic receptors recognise mannan from the pathogen surface and phosphatidylserine from end-life cells, respectively[39,40]. In order to reach particles, macrophages can migrate using mechanosensitive organelles, called podosomes, and following a chemokine ligand (CCL) 2 cytokine gradient[32,41].

All these receptors activate actin-polymerisation cascades, leading to modifications in the phagocyte surface and particle internalisation, creating the phagosome[39,40]. The latter is composed of pseudopods covering and isolating dangerous material[39].

Finally, repetition of fusion/fission phenomena with lysosomes containing proteolytic enzymes (*i.e.*, cathepsins, hydrolases) and acidic molecules helps the phagosome to mature into a phagolysosome and destruct its content[39,40]. Numerous proteins monitor the maturation, including several annexins, GTPases (guanosine triphosphate) and syntaxins[40].

However, some pathogens, notably *Salmonella*, *Legionella* and *Mycobacterium* genus, and malignant cells have evolved to survive inside macrophage phagosomes or to display CD47, as "don't eat me" signals to avoid engulfment[32,40,41].

2.3.2. Antigen presentation

AnPCs encompass DCs, macrophages and B-lymphocytes and embody cells able to downgrade exogenous pathogenic and self-antigens into minor peptides and display them on MHC-II molecules on their surface[31,39,42]. Although DCs are the most effective AnPCs, macrophages, but also monocytes, can create this signal required for T-cell activation and proliferation[32,39,42]. Accurately, the M1-phenotype mostly exerts AnPC functions on Th1 and Th17 through the production of IL-12 and IL-23[22].

Once the particle is phagocytized and digested, the variable α and β chains of MHC-II molecules are loaded into a stabilising and invariant chain in the endoplasmic reticulum before trafficking until AnPC surface[39,42,43]. Both processes are highly regulated respectively by IFN-γ and factors including cholesterol, kinases and GTPases, even though the question is still subject to debate among experts[39]. After interacting with TCR, MHC-II molecules are broken down via polyubiquitilation[39,43].

2.3.3. Cytokines production

Largely produced by macrophages and lymphocytes, cytokines are short-lived and low molecular weight hormones used for the intercellular communication of the immune system. Each of the 100 identified-cytokines respond to a specific stimulus, binds to a particular membrane receptor and positively or negatively regulates a signalling cascade that influences inflammation, metabolism, homoeostasis or tissue repair. Cytokines can be anti- or pro-inflammatory, and paracrine, autocrine or endocrine[44].

Macrophages cytokines influence their own polarisation, as explained above, but also trigger inflammation and activate the adaptative immune system[32,35,44]. Nonetheless, too much and too long cytokines production leads to sepsis shock and chronic inflammation, respectively. The former invokes an overwhelming release of TNF-α, IL-6 and IL-1β and can be lethal in

its final and immunosuppressive phase, while the latter implies CD163 accumulation, leading to uncontainable monocyte recruitment and metastasis[32,35].

2.4. TAMs

In cancer, although most macrophages present many M2-properties, expressing ARG-1, CD206 and low MHC-II molecules, research demonstrates that both M1- and M2-phenotypes can be found in TME, but also effectively intermediate phenotypes with shared characteristics, as the M1/M2 model remains limited (cf. 2.2. Activation pathways)[35,42]. Accordingly, TAMs can either combat tumours with a pro-inflammatory phenotype or promote their growth with anti-inflammatory features[42]. Key functions of anti-inflammatory TAMs in cancer development and proliferation will be mainly discussed below.

Firstly, via VEGF signalling, TAMs induce hypoxia and glycolysis, two factors driving angiogenesis, as well as vasculogenesis and lymphogenesis. Moreover, macrophages promote metastasis and tumour invasiveness with TGF-β secretion, while their granulins inhibit T-cell infiltration and TAM antigen presentation, lowering T-cell activation and proliferation afterwards. Furthermore, macrophages shape the immunosuppressive TME by ingesting metabolites, releasing anti-inflammatory cytokines and expressing immunosuppressive receptors. Finally, macrophagic mRNA can stimulate the chemotherapeutic resistance of cancerous cells, while irradiation favours M2-polarization[42]. Regarding those protumoral activities, ongoing studies are currently looking for an immunotherapy targeting TAMs[33].

In MPM, TAMs encounter for 27% of immune cells[12] and high TAM infiltration is correlated with worst OS in non-epithelioid subtypes[45,46]. TAM upregulation of IL-10 by tumour cells inhibits the immune response, while MPM cells tend to drive macrophages towards the M2-phenotype[18]. Moreover, asbestos fibres trigger macrophage TNF-α production, which stimulates cell proliferation and asbestos resistance in mesothelial cells[12].

2.5. Influence of the microenvironment

Among all microenvironmental factors influencing TAM polarisation and functions, fibroblasts, hypoxia and acidity are the prevailing ones, aside from T-cells. Other minor elements, including extracellular matrix (ECM), cellular debris, aerobic glycolysis and several pathways, will not be discussed due to poorer impacts[33,37].

Connective tissues are formed of fibroblasts that induce changes in the ECM. For instance, collagen manages macrophage polarisation into an M2-phenotype when integrin-linked periostin enhances TAM enrolment. Fibroblasts also regulate TAMs functions by surexpressing inflammatory cytokines, like GM-CSF, IL-6 and VEGF, and have indirect effects, disrupting nutrient and dioxygen availability[33].

Hypoxia, defining low oxygen concentration, emerges when malignant tumours spread speedily and induce TAM-favoured accumulation in those areas through monocyte-recruiting factors produced by tumoral and stromal cells. In some cancers, hypoxic TME promotes M2-phenotype polarisation and exosome secretion to impede immunity and improve metastasis and angiogenesis, enhancing tumour progression[33,37].

Acidity, mostly due to lactic acid, restrict polarisation to M2-macrophages and enhance monocarboxylate transporter activity. Besides, lysosome pH correlates with the M2-phenotype phagocytic role and may be a perspective of antitumoral treatment[33,37].

3. Eosinophils

Eosinophils are myeloid cells of the innate immune system and, alongside with basophils and neutrophils, form the subgroup of granulocytes[47], referring to their cytotoxic granules[31]. They are named after the pink colouration their granules take after eosin colouration and possess a bilobed nucleus[48]. Eosinophils are found in all vertebrate[49] and are mostly known for their anti-helminthic function and hypereosinophilia-linked diseases, *i.e.*, eosinophilic-asthma and allergy[48,50]. In blood, homeostatic eosinophil concentrations vary between 100 and 500 cells per µL[48,51,52].

3.1. Haematopoiesis and activation

Eosinophils originate from $CD34^+$ bone marrow HSC[48,53]. Three distinct steps can be defined: firstly, eosinophil progenitors (EoP) arise from common myeloid progenitors (CMP), shared precursors with basophils stemming from HSC. Then, a minute proportion of EoP enters the peripheral blood but most of them mature and gain granules in the bone marrow beforehand[48,53] (**Figure 6**). Once in the vasculature, mature eosinophils are recruited into tissues, mostly thymus, adipose tissue, uterus, gut, mammary glands and lungs[47,48,54]. However, with the recent advances in single-cell technologies, those earlier certainties have been called into question, reorganising the previous model with common GATA-1 axes, instead of the CMP[55,56].

Many cytokines and transcription factors are key for the eosinophilic lineage. CMP differentiation requires IL-3 and GM-CSF[54], while the transition to EoP is regulated by high levels of PU.1, synergically with GATA-1 and CCAAT/enhancer-binding protein (c/EBP)-α and -β[48,53,54,57]. Finally, IL-5 is the most specific cytokine for eosinophil maturation, expansion and survival, but also stimulates the spreading into the blood and the formation of granules[48,53,54]. Moreover, IL-3, IL-33 and GM-CSF also direct the maturation[48,53,54].

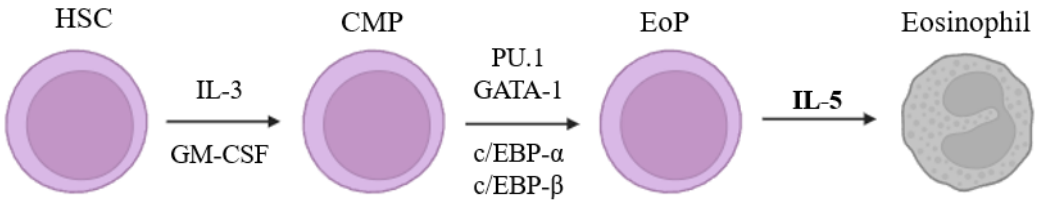

Figure 6 – **Haematopoiesis model for eosinophils**. The figure was created on the BioRender.com website.
Abbreviations : HSC, haematopoietic stem cells; CMP, common myeloid progenitor; EoP, eosinophil progenitor; IL, interleukine; GM-CSF, granulocyte-macrophage colony-stimulating factor; c/EBP, CCAAT/enhancer-binding protein.

3.2. Effector functions

3.2.1. Degranulation

A hallmark of eosinophil functions is degranulation, *i.e.*, the discharge of cytoplasmic granule content. Primary and secondary granules may be distinguished according to the crystalline core, present in the latter unlike the former[48,58]. Charcot-Leyden crystals (CLCs), compiled with CLC-protein or galectin-10, represent the predominant proteins in primary granules[48,58], while secondary are loaded with a vast range of basic proteins, namely eosinophil cationic protein (ECP), eosinophil peroxidase (EPO), major basic protein (MBP) and eosinophil-derived neurotoxin (EDN)[48,54,58].

The CLC-protein establishes bipyramidal hexagonal crystals[49,58,59] and possesses a high mannose-affinity structure[58,59]. A role in inflammatory response has been suggested as it stimulates cell migration and neutrophil extracellular trap (NET) formation[49].

For basic proteins, ECP belongs to the RNAse family and exerts antiviral, cellular and pro-apoptosis activities, *e.g.*, holing the target membrane. EPO represents 25% of the granules protein total mass and is able to catalyse oxidation, releasing ROS and RNI but also taking profit of hydrogen peroxide to nitrate proteins in an immune defence context. Besides, MBP, accounting for half of the granules protein total mass, expresses highly cytotoxic features against bacteria and parasites and is associated with tissue damage in asthma. For instance, MBP-1 possesses antiparasitic and antibacterial properties and stimulates mast cell functions. Finally, EDN is a poly-functional ribonuclease that activates DC- and Th2-associated immune responses.[48,49,54,58,60]

3.2.2. Regulation of the inflammation

As mature and non-dividing cells, eosinophils rapidly endure apoptosis in absence of IL-3, IL-5 and GM-CSF survival cytokines[48,61]. Apoptosis consists of cellular shrinking, DNA fragmentation and Annexin-V surface expression[48]. Siglec-8, CD69 and CD95 represent some of the receptors identified to favour the process once engaged[48,62], while IL-25, IL-33 and lymphopoietin delay it. In an inflammatory context, apoptosis can be used to resolve inflammation[48].

Concerning macrophages, eosinophils can trigger both M1- and M2-phenotypes by IFN-γ and IL-4 production, respectively, and hence, influence the inflammation[63,64].

3.2.3. Chemotaxis and adhesion

Chemotaxis refers to the phenomenon by which cells travel around the organism according to a chemokine gradient. The most powerful and selective chemokines for eosinophil

chemotaxis reside in eotaxins signalling through C-C chemokine receptor (CCR)-3, but CCL5, monocyte chemoattractant protein (MCP)-2,3 and 4 may also bind to this G-coupled protein receptor. Conversely, immunoglobulin-like receptor B will downregulate chemotactic responses[48].

Once the target location has been successfully reached, eosinophils need to adhere to the ECM for inter-tissular displacement. Cell surface molecules, such as integrins and selectins, are crucial for this mechanism. Integrins regulate ECM protein interaction, while selectins promote endothelium-eosinophil liaison. Moreover, IL-5 and eotaxin-1 attractant chemokines are known to favour integrins-ligand affinity[48].

3.3. Recruitment into the TME

Eosinophils migrate into the TME in response to three different kinds of stimuli[53]. Firstly, numerous cytokines and receptors are involved in the process, like chemoattractant fibroblasts-produced CCL11, CCL24 and CCL26[53], but also CCR3 which interacts with eotaxins[47,49,53]. IL-5, essential for eosinophil maturation, is also required in recruitment[47,53]. Then, HMGB1 and IL-33, two DAMPs, enhance eosinophil recruitment in hypoxic tumoral regions. IL-33 induces Th2 immune response and involves eosinophils through the receptor for advanced glycation end-products (RAGE) accessory protein, while HMGB1 stimulates CCL13 and CCL4 expression[53]. Finally, the microbiome may also play a role, as antibiotic treatment leads to microbial diversity diminishing and eosinophil infiltration[53].

3.4. Pleiotropy in cancer

Eosinophils are highly pleiotropic cells that can either favour or combat a tumour. In mice, TME-recruited eosinophils can be distinguished from tissue-resident ones[50,53].

Eosinophils can shape pro-tumoral TME through growth factor secretion, immune cell regulation and angiogenesis promotion[53]. Indeed, eosinophil endothelial growth factor (EGF) may provoke cancer expansion[65] and TGF-β1 can convert epithelial into mesenchymal histology in lung cancer[65,66], while eosinophil-derived CCL22 is known to enhance immunosuppressive Treg recruitment[67]. Furthermore, cervical tumour cells can produce lymphopoietin to stimulate VEGF production by eosinophils, which evokes new blood vessel formation[68]. Finally, eosinophils can catalyse the oxidative degradation of L-tryptophane and, hence, promote immunosuppressivity and impede T-cell response[69].

On the other hand, eosinophils exert direct and indirect antitumoral effects. For example, eosinophils have been proven to reduce tumoral growth, mainly through IL-10 and IL-12 secretion[70]. Via their granular proteins and soluble mediators, *e.g.*, IFN-γ[63,71], IL-5[63,71–73], IL-33[71], TNF[73] and CCL11[63,72], eosinophils can show direct cytotoxicity against cancer cells. Indeed, IFN-γ plays a key role in the complex antitumoral interaction between Treg, $CD8^+$ T-cells, M1-macrophages and eosinophils[63].

Regarding MPM, IL-5 absence has been demonstrated to decrease malignant pleural effusions[74], suggesting a pro-metastasis role of IL-5 in MPM, in murine models. In human, the correlation between eosinophil counts and shorter OS has been proven in chemotherapy treatment by the cellular and molecular epigenetic team[50].

PART II

MATERIAL & METHODS

II. MATERIAL & METHODS

4. Cell culture

Two distinct MPM cell lines were employed for this project : M14K (RRID:CVCL_8102) and ZL34 (RRID:CVCL_5906), respectively with epithelioid and sarcomatoid subtypes[75]. The culture was made with *Dulbecco's Modified Eagle Medium* (DMEM High glucose, Biowest), supplemented with 10% of heat-inactivated foetal bovine serum (FBS, Gibco) and 1% penicillin and streptomycin (10,000 units (U)/mL, PenStrep, Biowest). Phosphate-buffered saline (PBS, Biowest) and tryspin-ethylenediamine tetraacetic acid (EDTA, without Calcium and Magnesium, Biowest) were also used during cell culture, respectively to wash the flask and detach the cells.

5. Human primary cells

To isolate primary human immune cells, buffy coats from healthy donors of Red Cross of Belgium were used. This usage was approved by the institutional ethic committee of the Liège University hospital (Sart-Tilman) under the reference #2012/8. Blood, diluted twice with *Roswell Park Memorial Institute* (RPMI) 1640 with L-glutamine and 25mM Hepes (Biowest) supplemented with Penstrep 1%, was delicately discharged onto room temperature Lymphoprep (1.077 g/mL, Stemcell Technology) and centrifuged (MegaFuge 40R, Thermo Scientific) for 25 minutes at 400g (T_{room}; acceleration 6; deceleration 3). Plasma, peripherical blood mononuclear cells (PBMCs), polymorphonuclear (PMNs) and red blood cells (RBCs) were separated following a density gradient, as shown in **Figure 7**.

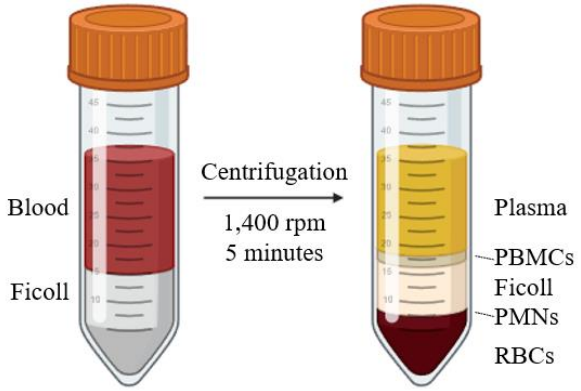

Figure 7 – **Blood separation through density gradient centrifugation**. PBMCs and PMNs were collected to isolate monocytes and eosinophils, respectively. The figure was created on the BioRender.com website.
Abbreviations : PBMC, peripherical blood mononuclear cells; PMN, polymorphonuclear; RBC, red blood cells.

5.1. Macrophages

5.1.1. Monocyte isolation and differentiation

The PBMCs ring was collected and washed with RPMI-PenStrep. After centrifugation (250g; 8 min; T_{room}), RBC lysis buffer (Bioscience), diluted 10 times with 0.2µm-sterile water, was used to break down the remaining RBCs. To limit the lysis, which activates immune cells, time was adapted (5, 8 or 10 minutes) depending on pellet redness. Lysis was stopped with PBS addition and cells were centrifuged (250g; 8 min; 10°C). Five cycles of washes with 35 mL of PBS and centrifugation (250g; 8 min; 10°C) were performed to remove cellular debris and plasma. Finally, cells were resuspended in RPMI, supplemented with 1% PenStrep, 2-mercaptoethanol (50µM, Gibco), Minimum Essential Medium Non-Essential Amino Acids (MEM NEAA 100X, Gibco) and sodium pyruvate **(**100 mM, Gibco**)**, counted with a Thoma-Zeiss counting chamber, seeded in 6-well plates (Greiner) (10.10^6 PBMCs/well, 2 mL) and incubated overnight to let monocytes adhere on the plate surface.

The following day, floating lymphocytes were removed with four washes of 2 mL of cold PBS and monocytes were cultured for 7 days in 2 mL of complete RPMI medium (supplemented with 1% PenStrep, 2-mercaptoethanol (50µM), MEM NEAA (1%), sodium pyruvate (100mM) and 10% FBS). Recombinant human (rh) M-CSF (Immunotools) was added with a 100 ng/mL final concentration to induce the differentiation into macrophages. After 3 days, monocytes were washed twice to remove floating cells and fresh complete RPMI medium supplemented with rhM-CSF was added.

5.1.2. Macrophage Polarisation

At the end of the differentiation, macrophages were washed twice, supplied with fresh complete RPMI medium and polarised or not with cytokines. To obtain naïve macrophages, termed M0, some wells were left unstimulated. To yield M1- and M2-macrophages, LPS (500 ng/mL, from *Escherichia coli* 055:B5, Sigma-Aldrich) and rhIFN-γ (20 ng/mL, Immunotools) or rhIL-4 (20 ng/mL, Immunotools) were respectively added for 48 hours.

5.2. Eosinophils

Eosinophil isolation and supernatant collection are routinely performed in the lab. Briefly, after PMN fraction collection from Lymphoprep-centrifuged blood, erythrocytes were lysed during cycles of 15-minutes incubation with RBC lysis buffer, PBS was added and cells were centrifuged (300g; 8 min; T_{room}; acceleration 6, deceleration 9). After a wash with 10 mL of PBS, granulocytes were counted and labelled with mouse IgG2a anti-human CCR3 (Fisher Scientific) diluted 1:100 in PBS, at 4°C for 30 minutes. After centrifugation (300g; 8 min; T_{room}; acceleration 6, deceleration 9) and supernatant removal, granulocytes were resuspended in MACS separation buffer (PBS-FBS 2%-EDTA 2mM) with anti-mouse IgG2a+b magnetic microbeads (1:4-ratio, MACS, Miltenyi Biotech) and incubated for 30 minutes. After two

washes with 4 mL of MACS separation buffer, cells were resuspended in the latter and positively selected by magnet isolation. Eosinophils, sticked to the tube walls due to the magnet attraction, were resuspended in a 1%-PenStrep-RPMI medium and seeded in T25 flasks. The next day, the culture medium was gathered and centrifuged (550g; 5 min; T_{room}). Eosinophils were removed through magnet isolation and supernatant was aliquoted, cooled at -20°C overnight and then stored at -80°C.

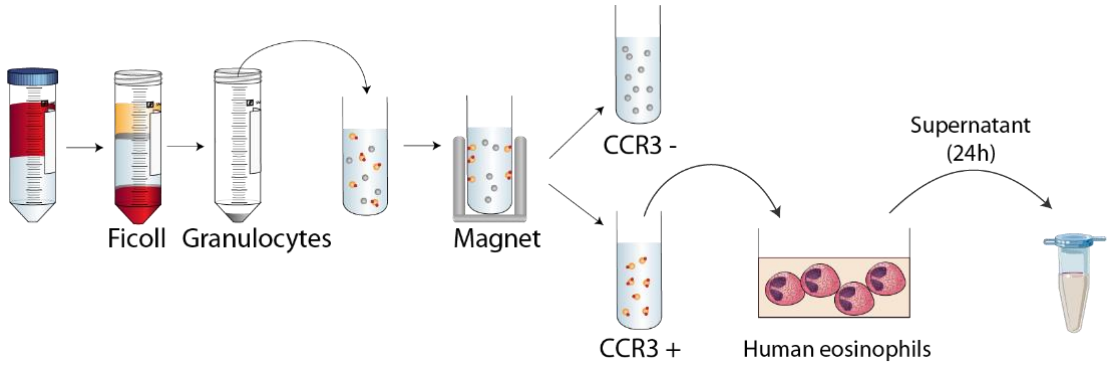

Figure 8 - **Experimental scheme of eosinophil supernatant production**.
*Abbreviation : CCR, C-C chemokine receptor*s.

6. Phenotype characterisation

M0-, M1- and M2-macrophages (cf. 2.1.2. Macrophages polarisation) were harvested with a scrapper and centrifuged (300g; 5 min; 10°C). Supernatant was removed and cells were resuspended in PBS-FBS 10% to block Fc receptors. After a 15 minutes incubation at 4°C, macrophages were centrifuged (550g; 4 min; 4°C) and resuspended in 50µL of PBS-FBS 2% and primary and coupled antibodies (**Tables 1a**) were added for a 45 minutes incubation at 4°C sheltered from light. After 30 minutes, CD80 and CD86 antibodies were added and incubated for the last 15 minutes. Cells were centrifuged and underwent two cycles of washes with 100µL of PBS-FBS 2% and centrifugation (550g; 4 min; 4°C). Secondary antibodies (**Table 1b**) diluted in PBS-FBS 2% were added and incubated for 30 minutes at 4°C sheltered from light. Cells were washed twice with PBS-FBS 2%, resuspended in 100µL of PBS-FBS 2% and analysed on the CytoFlex (Beckman Coulter) flow cytometer. Results were analysed with the CytExpert software (Beckman Coulter).

The same protocol was followed for MPM cells.

Table 1a – **Primary antibodies details**

Receptor	Conjugated fluorochromes	Isotype	Dilution (in PBS-FBS 2%)	Incubation time (min)	Supplier
CD80	Allophycocyanin (APC)	Mouse rIgG1	1:50	15	Miltenyi Biotec
CD86	VioBlue	Mouse rIgG1	1:50	15	Miltenyi Biotec
HLA-DR	Fluorescein isothiocyanate (FITC)	Mouse IgG2b	1:5	45	BD biosciences
CD206		Mouse IgG1	1:500	45	BD biosciences
PD-1	APC	Mouse IgG1	2:5	45	BD biosciences
PD-L1	APC	Mouse IgG1	1:100	45	BD biosciences

Table 1b – **Secondary antibodies details**

Receptor	Conjugated fluorochromes	Isotype	Dilution (in PBS-FBS 2%)	Incubation time (min)	Supplier
CD206	FITC	Goat anti-mouse IgG1	1:1000	30	Invitrogen

7. Cytotoxicity assays

7.1. CFSE-staining

After culture (cf. 1. Cell culture), MPM cells were washed once with PBS (10 mL), counted and resuspended at a 2.10^6 cells/mL in DMEM, supplemented with 1% PenStrep. Carboxyfluorescein succinimidyl esters (CFSE, Biorad) was added at a 10µM and 20µM final concentration, for M14K and ZL34, respectively. After 20 minutes of incubation at 37°C sheltered from light, cells were centrifuged, washed with PenStrep DMEM (4.10^5 cells/mL), centrifuged again (300g, 5 min, T_{room}) and resuspended in complete DMEM. CFSE-stained-cells were seeded in 100µL of complete-DMEM on flat-bottom 96-well plates (Greiner) (**Table 2**). To evaluate MPM cells autofluorescence, three wells were seeded with unlabelled cells. Plates were incubated for 3 hours to allow cell adhesion.

Table 2 – **Number of MPM cells according to ratios and cells lines**

Cell lines	M14K	ZL34
Total number of cells/well	5,000	4,000
MPM cells only	5,000	4,000
Ratio 1:1	2,500	2,000
Ratio 3:1	3,750	3,000

7.2. IncuCyte

50µL of human eosinophil supernatant (HE SN) or RPMI-PenStrep were added in the 96-well plates. Macrophages were incubated 15 minutes in RPMI-EDTA 10mM and recovered with gentle scrapping. After centrifugation, M0-, M1- and M2-macrophages (cf. 2.1.2. Macrophages polarisation) were resuspended in 1 mL of RPMI supplemented with 10% FBS, 1% PenStrep and 100mM sodium pyruvate and counted with Thoma-Zeiss counting chamber. Macrophages were diluted in complete-RPMI depending on ratios (**Table 3**) and 50µL was added in each well. Anti-PD-1 blocking antibody (10 µg/mL, InVivoMAb) and 5µL of AnnexinV-APC (Immunotools) were added in wells. Plates were placed in the IncuCyte S3 Live-Cell (Sartorius) imagery system, furnished with 37°C and 5% CO_2 incubator. Acquisition was realised every 2 hours for 50 hours. The percentage of apoptotic MPM cells was determined with the IncuCyte 2023A software. Cells were discriminated based on parameters listed in **Table 4**.

Table 3 – **Number of macrophages according to ratios and cells lines**

Cell lines	M14K	ZL34
Total number of cells/well	5,000	4,000
MPM cells only	0	0
Ratio 1:1	2,500	2,000
Ratio 3:1	1,250	1,000

Table 4 – **IncuCyte acquisition and analysis parameters**

Parameters	M14K	ZL34	AnnexinV+ cells
Channel	Green	Green	Red
Acquisition time (ms)	250	250	400
Threshold	0.5000	0.5000	1.0000
Edge split	Off	Off	Off
Hole fill (µm²)	50.00	0.0000	100.00
Minimum area (µm²)	100.000	100.000	50.000

8. Analysis

Flow cytometry results were analysed with CytExpert software. Percentage of deaths from IncuCyte analysis was calculated on the Excel software. Histograms and graphs were shaped with FlowJo vX.0.7 and GraphPad Prism 8.4.3. software, respectively. Most figures were realised on BioRender website.

Statistical analysis was performed on GraphPad Prism 8.4.3. software. Normality was assessed through Shapiro-Wilk test. The means of distributions were compared with an ordinary one-way ANOVA, followed by a multiple comparison test of Tukey. Data are expressed as mean +/- standard deviation (SD).

PART III

RESULTS

III. RESULTS

9. Primary macrophages culture

Human primary PBMCs were isolated through a density gradient and incubated overnight. Floating lymphocytes were removed and monocytes were differentiated into macrophages for 7 days in M-CSF-supplemented medium. For 48 hours, macrophages were polarised into the M1- and M2-phenotypes by complementing the medium with IFN-γ and LPS or IL-4, respectively (**Figure 9A**), to be used in the following experiments. To keep traces of cell morphology, images were taken after monocyte isolation (**Figure 9B**), differentiation (**Figure 9C**) and macrophage polarisation (**Figure 9D-F**) with a microscope (Revolve, Discover Echo).

As visible on **Figure 9B-F**, each culture step may be distinguished by cell morphology. Indeed, monocytes gain in size throughout differentiation. Besides, M1-polarization alters the round-shaped of the M0-phenotype into a more elongated cell, while M2-polarized cells tend to get bigger, within the limits of surface availability. M0-macrophages culture was more heterogenous and no distinction between before and after the 48 hours polarisation can be made, as no stimulus was added.

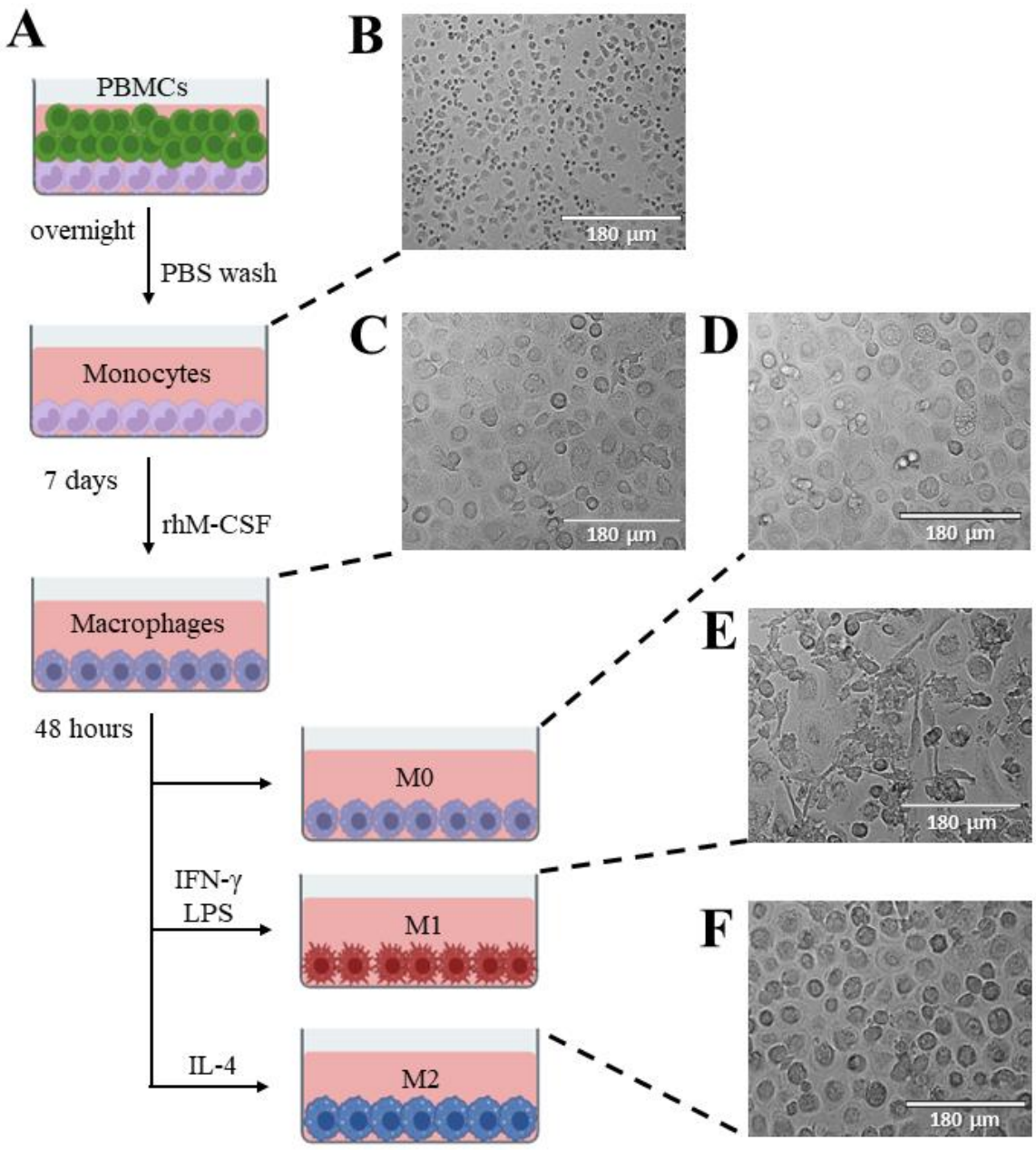

Figure 9 – **Differentiation and polarisation of primary human macrophages**. (**A**) **Experimental scheme**. PBMCs, collected on Ficoll, were seeded and incubated overnight. T-lymphocytes were removed from monocytes through PBS washes. M-CSF was added to differentiate monocytes into macrophages for 7 days. Macrophages were incubated with IFN-γ and LPS or IL-4 for 48 hours for polarisation into the M1- and M2-phenotypes, respectively. The scheme was created on the BioRender.com website. (**B**) **Monocytes** after PBS washes. (**C**) **Macrophages** after 7 days of differentiation. (**D**) **M0-macrophages** after 48 hours of unstimulation. (**E**) **M1-macrophages** after 48 hours of IFN-γ and LPS stimulation. (**F**) **M2-macrophages** after 48 hours of IL-4 stimulation. Images were acquired with a microscope (Revolve, Discover Echo).

Abbreviations : PBMC, peripherical blood mononuclear cells; M-CSF, macrophage colony-stimulating factor; IFN, interferon; LPS, lipopolysaccharides; IL, interleukin.

10. Membrane receptors characterisation

10.1. Gating strategy for macrophages

Human primary M0-, M1- and M2-macrophages were recovered by gentle scrapping. Separate staining with propidium iodide (PI, Enzo) and Zombie Aqua (BioLegend) was performed. The former is a DNA intercalating dye excluded by intact cell membrane[76,77] and the latter reacts with primary amine groups on proteins. In living cells, the dye is excluded and only labels surface proteins. When Zombie Aqua enters the death cell cytoplasm, it can react with a larger amount of proteins, which increases the signals[78]. To minimise the potential macrophage phagocytosis, PI staining has been realised at the latest moment before analysis, while Zombie Aqua needs a 30 minutes incubation. Cells were analysed through flow cytometry on the CytoFlex (**Figure 10A**).

Results (**Figure 10B**) were analysed on CytExpert software. At first, a graph presenting forward versus side scatters (FSC and SSC, orange population), standing for cell height and granularity, respectively, was considered. Two cell populations can clearly be distinguished based on those morphological features. To discern the deceasing-cell population, the two mortality markers, PI and Zombie Aqua, were employed. PI^+ and Zombie $Aqua^+$ cells can be observed on graphs presenting fluorescence intensity versus FSC (**Figure 10B**). Finally, a comeback to the FSC versus SSC graphs (**Figure 10B**) highlights PI^+ and Zombie $Aqua^+$ populations as the left ones (purple for PI, green for Zombie Aqua).

Following those statements, the gating strategy as in **Figure 10C** was adopted for all subsequent flow cytometry experiments on primary macrophages. First, a population was delineated on FSC/SSC graph to isolate living cells. Then, on a FSC-A/FSC-H (respectively area and height) graph showing only previously gated population, singlets were selected by circumscribing the concentrated population. Afterwards, doublets, *i.e.*, two sticked-cells detected together, display a doubled area for the same height as singlets.

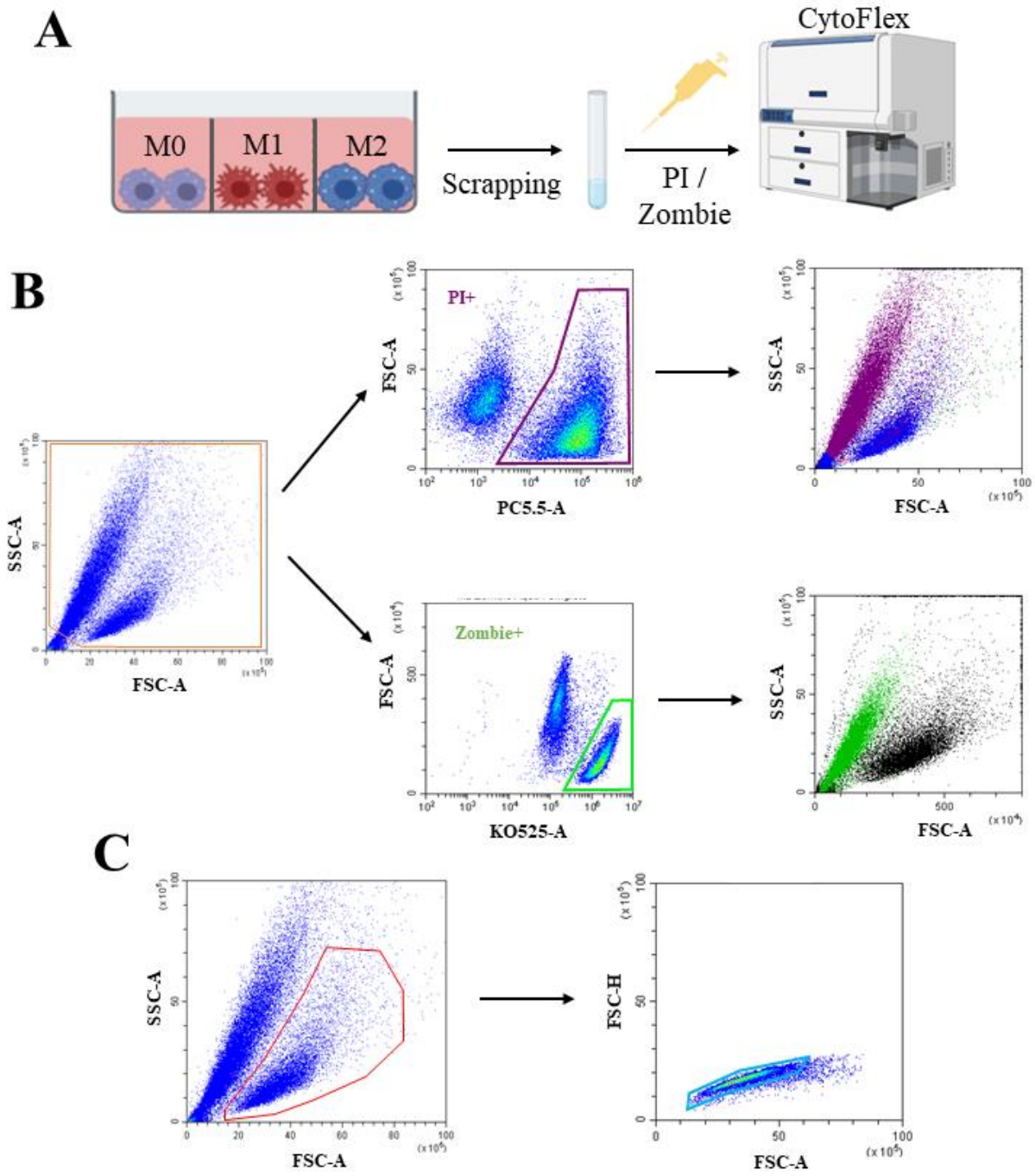

Figure 10 – **Gating strategy for macrophages**. (**A**) **Experimental scheme**. Primary human M0-, M1- and M2-macrophages were scrapped and PI (at a final concentration of 4µg/mL) or ZombieAqua (diluted 1:250) was added. Cells were analysed by flow cytometry (CytoFlex) and the CytExpert software was used for data analysis. The scheme was created on the BioRender.com website. (**B**) **Identification of living and dead cells**, based on FSC/SCC profiles of PI^+ and $ZombieAqua^+$ cells. (**C**) **Gating strategy**.
Abbreviations : PI, propidium iodide; FSC, forward scatter; SSC, side scatter.

10.2. Expression of membrane-associated receptors

To characterise their polarisation, primary human macrophages with the M0-, M1- and M2-phenotypes were stained with anti-**CD80**, -**CD86**, -**HLA-DR**, -**CD206**, -**PD-1** and -**PD-L1** antibodies and analysed by flow cytometry (**Figure 11A**). CD80 and CD86 are expressed by AnPCs to activate T-lymphocytes[12,18]. CD206, mostly known as mannose receptor, can recognise mannan from pathogen cell surface[40], while HLA-DR is an MHC class II molecule and mediates antigen presentation[79]. Furthermore, PD-1 and its ligand, PD-L1, are both expressed by M1- and M2-macrophages and play a role in T-cell anergy and enhance tumour immune escape[29,80].

To visualise the expression profiles and intensities, histograms were extracted from FlowJo vX.0.7. for the six markers (**Figure 11B**). Isotype controls are shown to indicate the baseline and confirm the absence of aspecific signal. **CD80** is highly expressed by the M1-phenotype and by a portion of M0- and M2-macrophages, while **CD86** is hardly expressed by the M1- and M0-phenotypes, but by a fraction of M2-macrophages. Besides, **HLA-DR** is more expressed on M2- and M0-populations than on the M1-one, while **CD206** receptor is mostly displayed by the M2-phenotype. Regarding **PD-1** and **PD-L1**, macrophages hardly express the former, while the latter is decreasingly displayed by M1-, M2- and M0-macrophages.

Besides, results were analysed with the CytExpert software and the relative median fluorescence intensity (rMFI) of each receptor was calculated by dividing the MFIs of stained samples by the control one (**Figure 11C**). Although highly variable, the **CD80** receptor is highly expressed by M1-macrophages, which differs significantly with the M0- and M2-phenotypes (both p-values < 0.0001). Despite the high results variability, the **CD86** receptor is more expressed by M2-macrophages, in comparison to the M1-phenotype (p-value = 0.0478).

Moreover, **HLA-DR** is highly expressed by M0- and M2-macrophages, with no significant difference between the two (p-value = 0.9910), while the M1-phenotype hardly expresses it ($p_{M0\text{-}M1} = 0.0045$ and $p_{M1\text{-}M2} = 0.0036$). Even if data are fluctuating, M2-macrophages display an extensive expression of **CD206** ($p_{M0\text{-}M2} = 0.0002$ and $p_{M1\text{-}M2} = 0.0001$), but none for the M0- and M1-phenotypes ($p_{M0\text{-}M1} = 0.9466$).

Finally, results for **PD-1** are largely variable and nonsignificant ($p_{M0\text{-}M1} = 0.9428$, $p_{M0\text{-}M2} = 0.9909$ and $p_{M1\text{-}M2} = 0.9784$), while **PD-L1** is intensely expressed by M1- and M2-macrophages, but to a lesser extent for the latter ($p_{M1\text{-}M2} = 0.0027$), while M0-macrophages hardly express the ligand ($p_{M0\text{-}M1} = <0.0001$ and $p_{M0\text{-}M2} = 0.0261$).

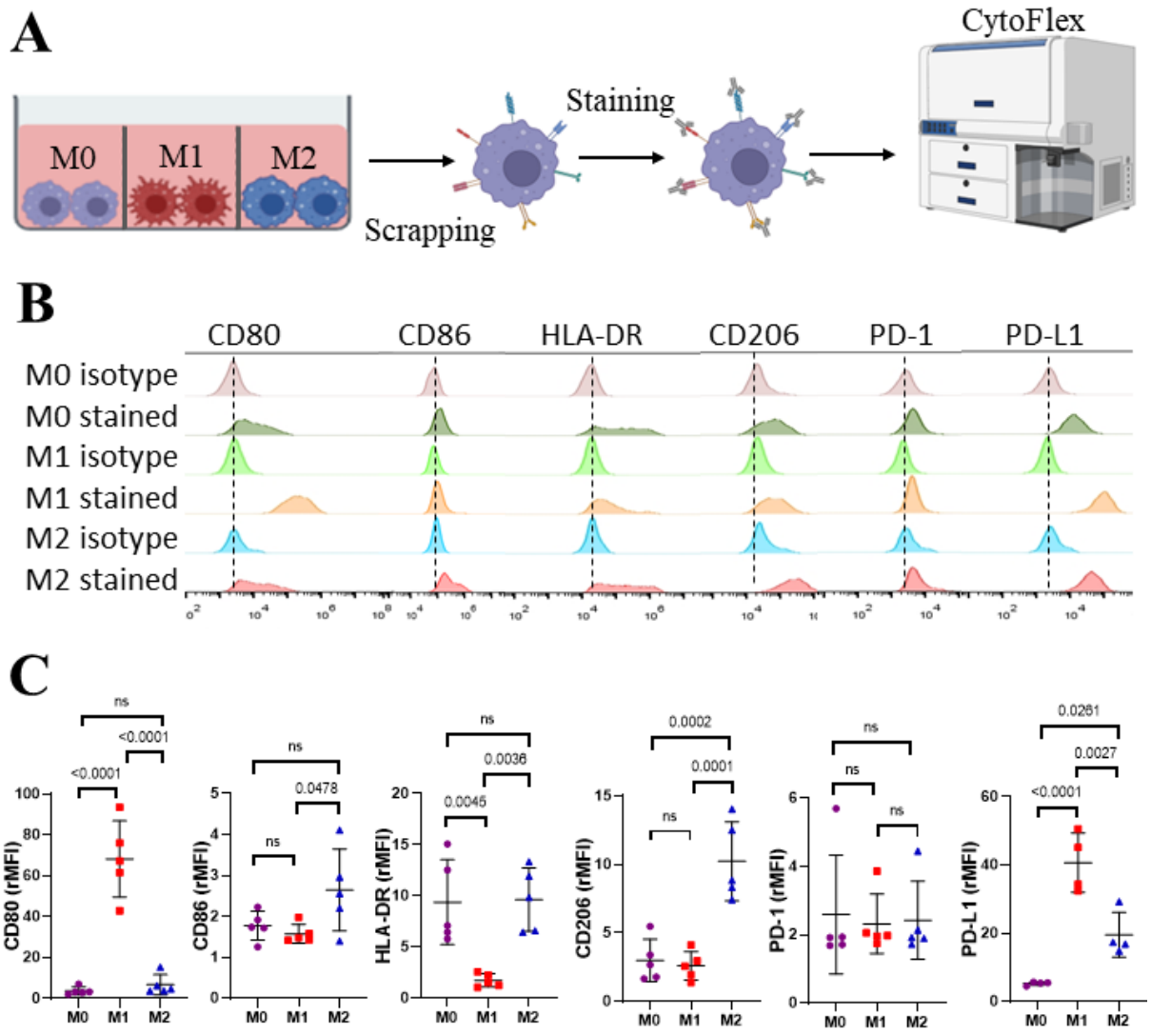

Figure 11 – **Macrophages phenotype**. (**A**) **Experimental scheme**. Macrophages were collected with a scrapper. After Fc receptors blocking, cells were labelled with anti-CD80, -CD86, -HLA-DR, -CD206, -PD-1 and -PD-L1 antibodies. Cells were analysed by flow cytometry (CytoFlex). The scheme was created on the BioRender.com website. (**B-C**) **Surface expression** of CD80, CD86, HLA-DR, CD206, PD-1 and PD-L1. Graphs were generated with FlowJo vX.0.7 and GraphPad Prism 8.4.3, respectively. The rMFI corresponds to the ratio of the MFI of the surface markers with their control. Data are expressed as mean +/- SD, each point representing an independent test. Statistics were realised on GraphPad Prism 8.4.3. with a Shapiro-Wilk test to assess the normality and a one-way ANOVA, followed by a Tukey's multiple comparison test.

Abbreviations : Fc, fragment crystallisable; CD, cluster of differentiation; HLA, human-leukocyte antigen; PD, programmed cell death; PD-L, PD-ligand; rMFI, relative median fluorescence intensity; SD, standard deviation.

10.3. Modulation of PD-1 and PD-L1 expression by eosinophils

10.3.1. Macrophages

After 48 hours of culture in medium supplemented with 25% (v:v) of HE SN, primary human M0-, M1- and M2-macrophages were stained with anti-PD-1 and anti-PD-L1 antibodies (**Figure 12A**).

To visualise the expression profiles and intensities, histograms were extracted from FlowJo vX.0.7. for the two markers (**Figure 12B**). Isotype controls are shown to indicate the baseline and confirm the absence of aspecific signal. **PD-1** seems to be expressed, as stained samples show higher fluorescence than isotype controls. Besides, **PD-L1** expression is enhanced in M1- and M2-macrophages, especially the M1-phenotype before HE SN co-culture. However, for both, no visual distinction can undoubtedly be made without rMFI values.

Likewise, results were analysed with the CytExpert software and the rMFI of each receptor was calculated by dividing the MFIs of stained samples by the control one. Results for **PD-1** (**Figure 12C**) antibody are highly variable and non-significant, both between macrophage types after 48 hours of HE SN supplemented-medium culture ($p_{M0\text{-}M1}$ = >0.9999 , $p_{M0\text{-}M2}$ = 0.9998 and $p_{M1\text{-}M2}$ = 0.9999) and before and after the supplemented-culture (p_{M0} = 0.9171, p_{M1} = 0.9960 and p_{M2} = 0.9228). Meanwhile, **PD-L1** expression (**Figure 12D**) by the M1-phenotype decrease after the culture with HE SN (p-value = <0.0001). Even if non-significant, M2-macrophages tend to have a lower PD-L1 expression after the supplemented-culture (p-value = 0.0815), while the M0-phenotype expression does not change (p-value = >0.9999). In this way, even if PD-L1 expression differs in macrophage subtypes before supplementing the culture (cf. 10.2. Expression of membrane-associated receptors, $p_{M0\text{-}M1}$ = <0.0001, $p_{M0\text{-}M2}$ = 0.0261 and $p_{M1\text{-}M2}$ = 0.0027), the decrease after 48 hours makes the difference nonsignificant after the HE SN supplemented-culture ($p_{M0\text{-}M1}$ = 0.2569, $p_{M0\text{-}M2}$ = 0.4757 and $p_{M1\text{-}M2}$ = 0.9992).

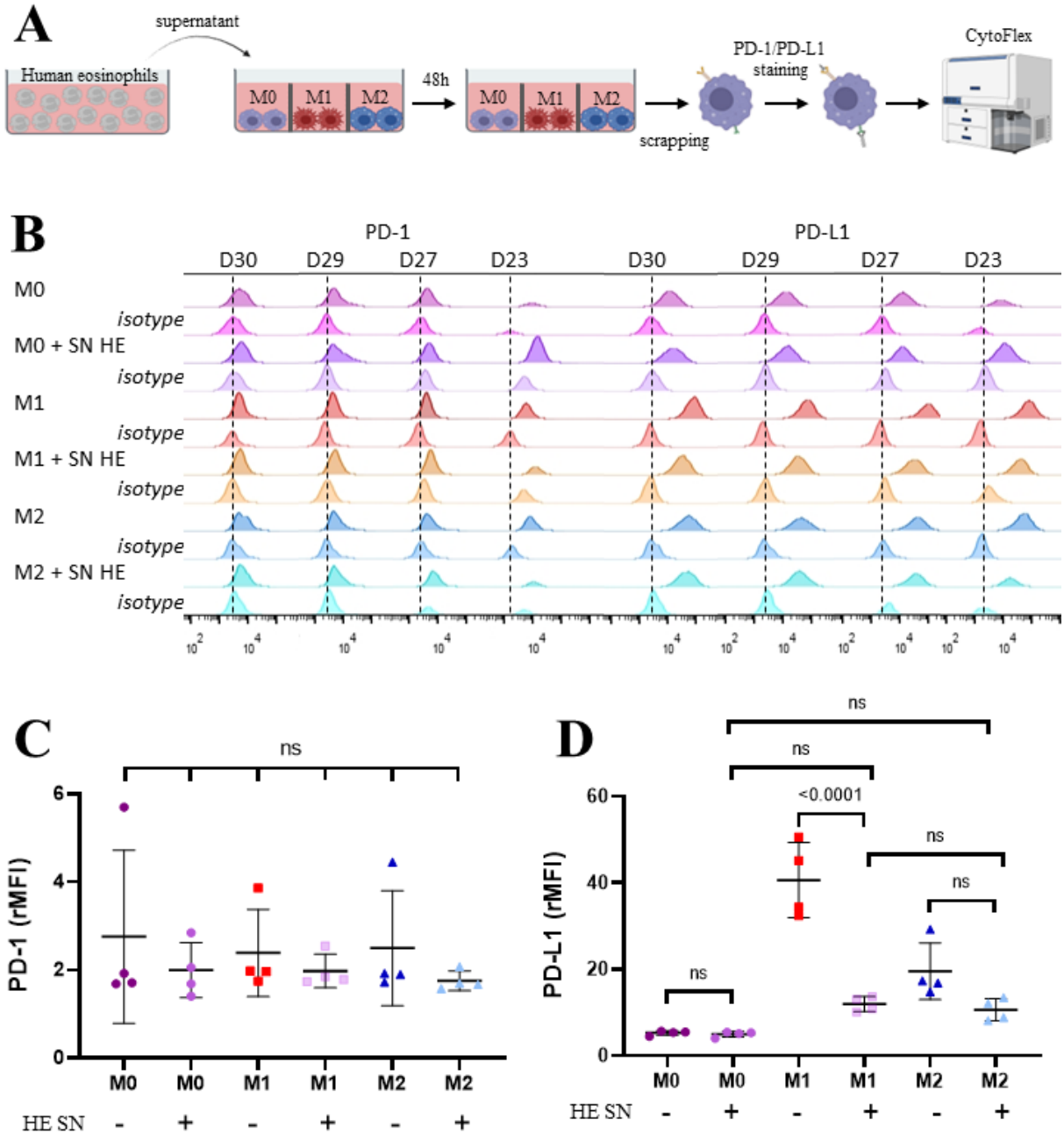

Figure 12 – **Impact of human eosinophil supernatant on PD-1/PD-L1 expression of macrophages**. (**A**) **Experimental scheme**. After polarisation, macrophages were cultured in RPMI supplemented with 25% (v:v) of HE SN. After 48 hours of incubation and Fc receptor blocking, cells were labelled with anti-PD-1 and anti-PD-L1 antibodies. Cells were analysed by flow cytometry (CytoFlex). The scheme was created on the BioRender.com website. (**B**) **Surface expression** of PD-1 and PD-L1 for each donor. Histograms were generated with FlowJo vX.0.7. The rMFI for PD-1 (**C**) and PD-L1 (**D**) corresponds to the ratio of the MFI of the surface markers with their control. Graphs were obtained with GraphPad Prism 8.4.3. Data are expressed as mean +/- SD, each point representing an independent test. Statistics were realised on GraphPad Prism 8.4.3. with a Shapiro-Wilk test to assess the normality and a one-way ANOVA, followed by a Tukey's multiple comparison test.
Abbreviations : PD, programmed death cell; PD-L, PD-ligand; RPMI, Roswell Park Memorial Institute; HE SN, human eosinophil supernatant; Fc, fragment crystallisable; rMFI, relative median fluorescence intensity; SD, standard deviation.

10.3.2. MPM cells

After 48 hours of culture in medium supplemented with 25% (v:v) of HE SN, ZL34 and M14K were stained with anti-PD-1 and anti-PD-L1 antibodies (**Figure 13A**).

To visualise the expression profiles and intensities, histograms were extracted from FlowJo vX.0.7. for the two markers (**Figure 13B**). Isotype controls are shown to indicate the baseline and confirm the absence of aspecific signal. Both **PD-1** and **PD-L1** are expressed by MPM cell lines, with a higher MFI for the latter. However, for both, no visual distinction can undoubtedly be made without rMFI values.

Likewise, results were analysed with the CytExpert software and rMFI of each receptor was calculated by dividing the MFIs of stained samples by the control one (**Figure 13C**). Results for **PD-1** antibody are quite variable, but no change in expression has been observed ($p_{M14K\ mock/HE\ SN} = 0.9545$, $p_{ZL34\ mock/HE\ SN} = 0.8051$, $p_{mock\ M14K/ZL34} = 0.7733$ and $p_{HE\ SN\ M14K/ZL34} = 0.9675$). **PD-L1** expression tends to lower in M14K culture with the HE SN, even if not significant (p-value = 0.5372) and remain constant for ZL34 (p-value = 0.9877).

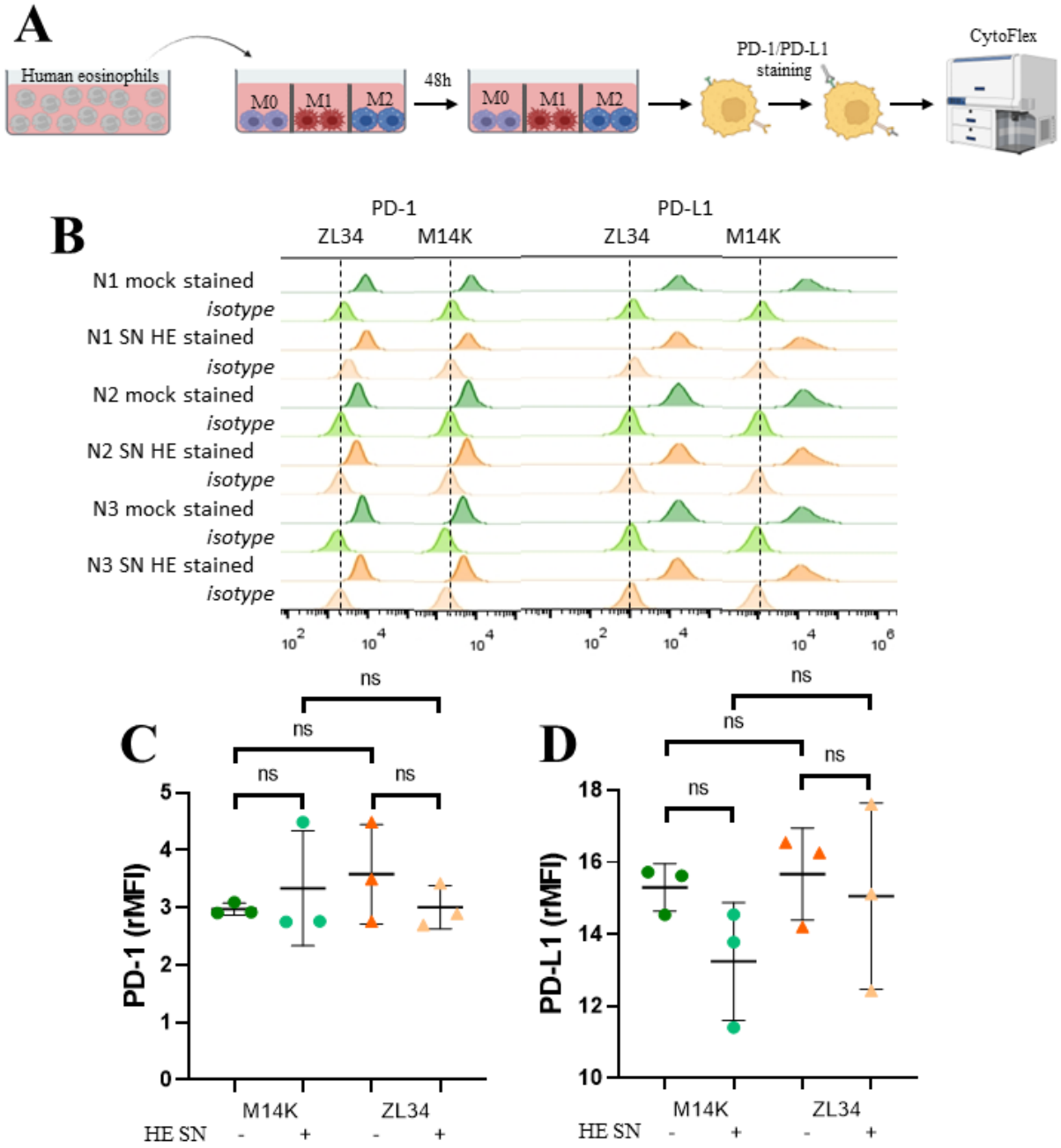

Figure 13 – **Impact of human eosinophil supernatant on PD-1/PD-L1 expression of MPM cells**. (A) **Experimental scheme**. M14K and ZL34 cell lines were cultured or not (mock) with 25% (v:v) of HE SN for 48 hours. Cells were collected, labelled with PD-1 and PD-L1 and analysed by flow cytometry (CytoFlex). The scheme was created on the BioRender.com website. (**B**) **Surface expression** of PD-1 and PD-L1. Histograms were generated with FlowJo vX.0.7. The rMFI for PD-1 (**C**) and PD-L1 (**D**) corresponds to the ratio of the MFI of the surface markers with their control. Graphs were obtained with GraphPad Prism 8.4.3. Data are expressed as mean +/- SD, each point representing an independent test. Statistics were realised on GraphPad Prism 8.4.3. with a Shapiro-Wilk test to assess the normality and a one-way ANOVA, followed by a Tukey's multiple comparison test.

Abbreviations : PD, programmed death cell; PD-L, PD-ligand; MPM, malignant pleural mesothelioma; HE SN, human eosinophil supernatant; rMFI, relative median fluorescence intensity; SD, standard deviation.

11. Mortality assessment in MPM-macrophages co-culture

11.1. Cytotoxicity of primary macrophages towards MPM cells

To evaluate the impact of eosinophil cytokines on macrophage cytotoxicity, MPM cells (ZL34 and M14K cell lines) were labelled in green with CFSE and cultured with M0-, M1- or M2-macrophages in a MPM-to-macrophage ratio of either 1:1 or 3:1. HE SN, anti-PD1 and AnnexinV-APC, an APC-conjugated dye binding specifically on phosphatidylserine exposed on apoptotic cell membranes[81], were successively added. Acquisitions were taken every 2 hours for 50 hours on the IncuCyte S3 Live-Cell (Sartorius) (**Figure 14A**).

As an example, a representative image of MPM cells dying can be found in **Figure 14B**. At the beginning of the co-culture, MPM cells, stained in green, adhere to the plate surface. After a certain hour (16 hours in this example), the nucleus start being coloured red. Red-labelling expands to the whole cell and, finally, MPM cells shrink and get rounded.

Analyses were performed on the IncuCyte 2023A software from Sartorius. Green and red parameters were carefully selected to suit every condition and timing. Data were exported and the division of MPM death cells (*i.e.*, green and red) by all MPM cells (*i.e.*, green) was done on Excel.

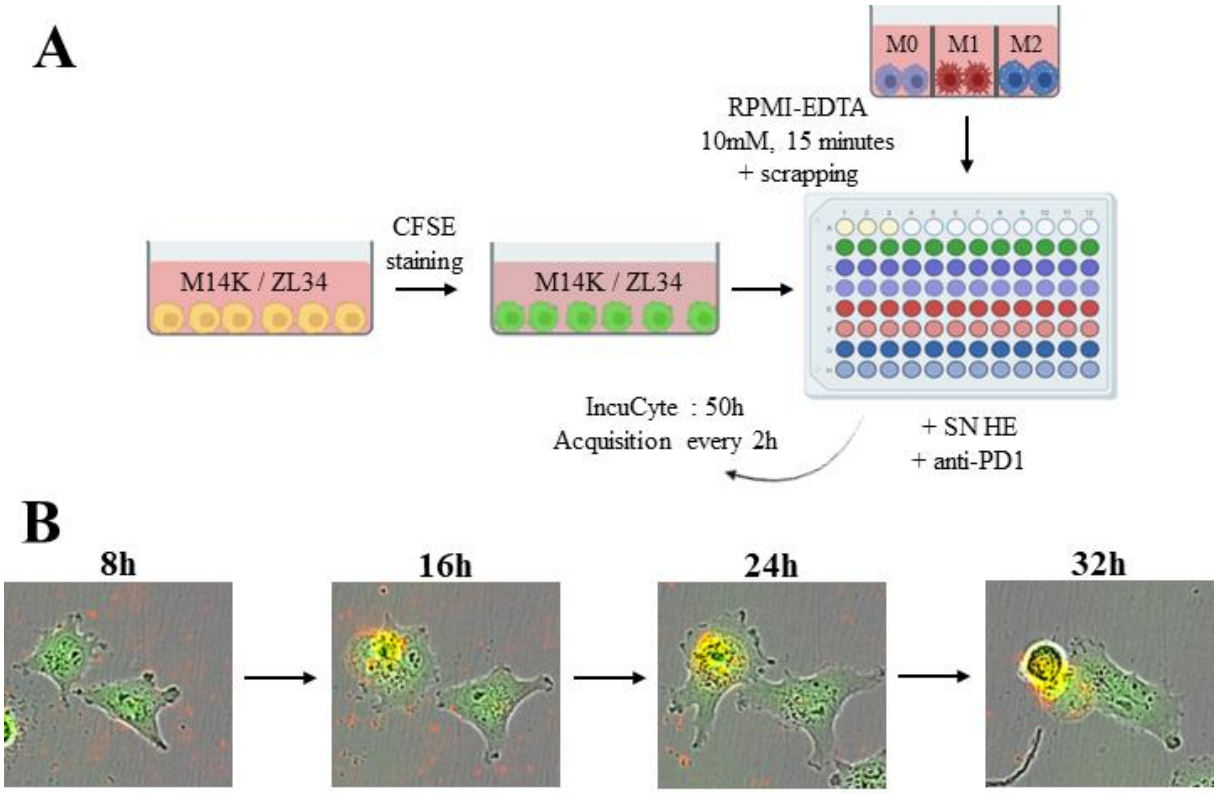

Figure 14 – **Cytotoxicity of primary macrophages towards MPM cells**. (**A**) **Experimental scheme**. CFSE-stained MPM cells (green) were co-cultured with M0-, M1- and M2-macrophages in a 1:1 and 3:1 ratio. SN HE (25% v:v) and/or anti-PD-1 (10µg/mL) were added to the culture medium. Co-culture was labelled with AnnexinV-APC and monitored with the IncuCyte S3 Live-Cell (Sartorius) every 2 hours for 50 hours. The scheme was created on the BioRender.com website. (**B**) **Representative image of an AnnexinV-APC^{+} MPM dying cell**.

Abbreviations : RPMI, Roswell Park Memorial Institute; EDTA, Ethylenediamine tetraacetic acid; CFSE, carboxyfluorescein succinimidyl ester; HE SN, human eosinophil supernatant; PD, programmed death cell; MPM, malignant pleural mesothelioma; APC, allophycocyanin.

11.1.1. ZL34 cell line

Apoptotic rates of ZL34 (**Figure 15A**), the sarcomatoid cell line[75], were established for co-culture with macrophages in a 1:1 ratio with the M0-, M1- and M2-phenotypes (**Figures 15B, D and F**, respectively) and in a 3:1 ratio with the M0-, M1- and M2-phenotypes (**Figures 15C, E and G**, respectively).

For all conditions, the mortality rate tends to increase over time. Even if nothing is significant, some tendencies can be highlighted. Conditions with anti-PD-1^+ and HE SN^+ display a higher lethality, followed by anti-PD-1^+ SN HE^- ones, while the anti-PD-1^- SN HE^+ wells have cells that tend to survive longer. Moreover, MPM cells without macrophages exhibit an increased survival rate, while co-culture with the M1-phenotype shows a higher mortality percentage, followed by co-culture with the M0-macrophages. Also, for those previous phenotypes, the MPM-to-macrophage ratio 1:1 seems to have an enhanced mortality rate, unlike M2-macrophages co-culture.

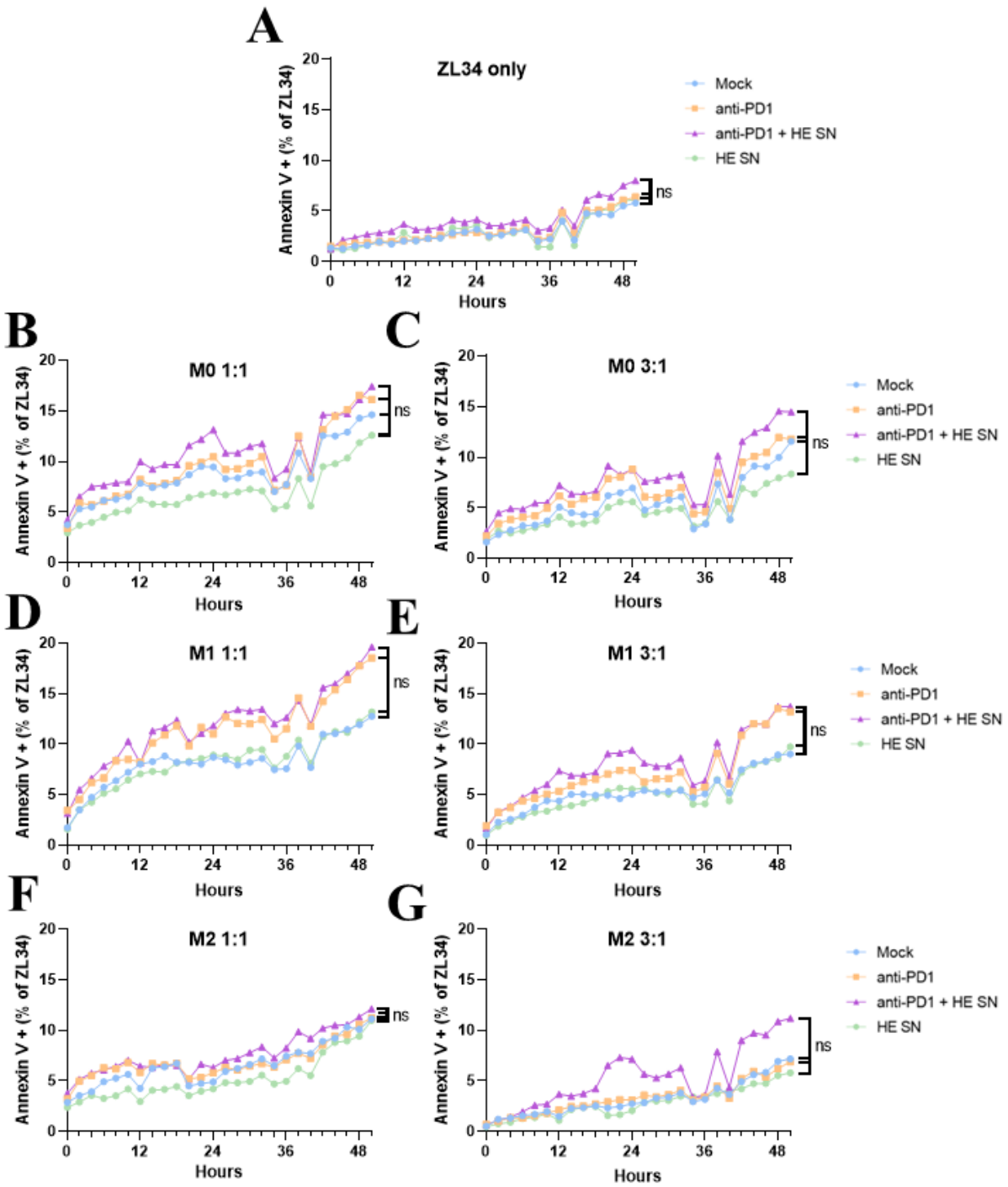

Figure 15 – **Time-lapse cytotoxicity of primary macrophages towards ZL34 cells**. Apoptotic rates of ZL34 cells ($CFSE^+AnnexinV\text{-}APC^+$) (**A**) co-cultured in 1:1 ratio with M0- (**B**)**,** M1- (**D**), M2-macrophages (**F**) or in a 3:1 ratio with M0- (**C**)**,** M1- (**E**), M2-macrophages (**G**) in presence or not of 25% (v:v) of HE SN and/or anti-PD-1. Results are expressed as the mean of intensity of each donor (N=2). Each donor was analysed in triplicate. Graphs were obtained with GraphPad Prism 8.4.3. Data are expressed as mean +/- SD, each point representing an independent test. Statistics were realised on the 50h data on GraphPad Prism 8.4.3. with a Shapiro-Wilk test to assess the normality and a one-way ANOVA, followed by a Tukey's multiple comparison test.

Abbreviations : CFSE, carboxyfluorescein succinimidyl ester; HE SN, human eosinophil supernatant; PD, programmed death cell.

11.1.2. M14K cell line

Apoptotic rates of M14K (**Figure 16A**), the epithelioid cell line[75], were established for co-culture with macrophages in a 1:1 ratio with the M0-, M1- and M2-phenotypes (**Figures 16B, D and F**, respectively) and in a 3:1 ratio with the M0-, M1- and M2-phenotypes (**Figures 16C, E and G**, respectively).

For all conditions, the mortality rate tends to increase over time. Except for M0-macrophages, ratio 1:1, anti-PD-1^+ and HE SN^+ wells (p-value = 0.0026), no significant differences can be found, but some tendencies can be highlighted. Wells containing only MPM cells display a higher survival rate, while wells with M0- or M1-macrophages exhibit a higher mortality percentage. Moreover, for the M1-phenotype with a 3:1 ratio, conditions with anti-PD-1^+ and HE SN^+ show a higher mortality rate ($p_{mock/anti\text{-}PD\text{-}1+,HE\ SN+} = 0.9473$), just as the M1-phenotype with a 1:1 ratio, anti-PD-1^- and HE SN^+ (p-value = 0.1023), followed by anti-PD-1^+ and HE SN^+ conditions (p-value = 0.3575).

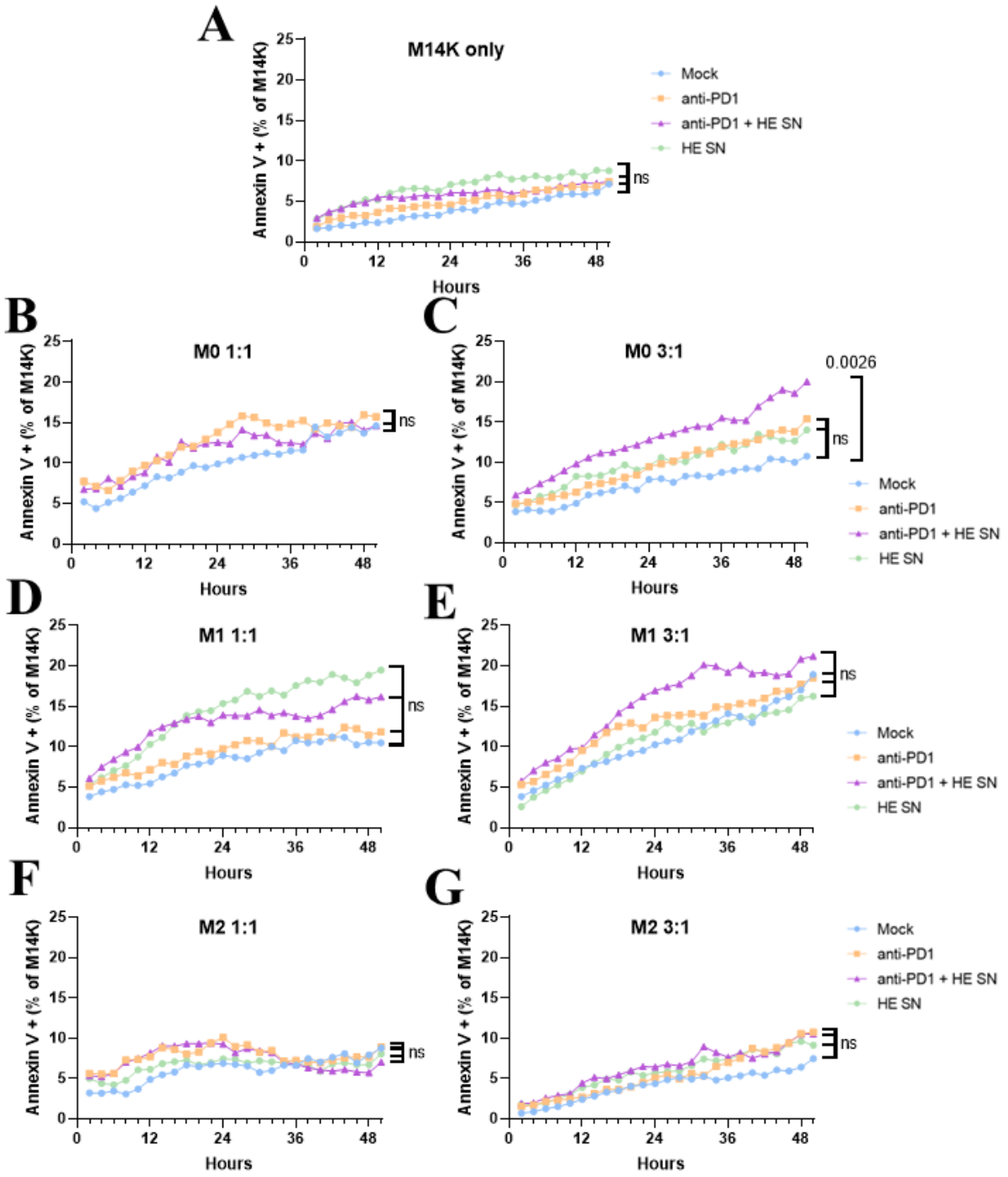

Figure 16 – **Time-lapse cytotoxicity of primary macrophages towards M14K cells**. Apoptotic rates of M14K cells ($CFSE^+AnnexinV\text{-}APC^+$) (**A**) co-cultured in a 1:1 ratio with M0- (**B**)**,** M1- (**D**), M2-macrophages (**F**) or in a 3:1 ratio with M0- (**C**)**,** M1- (**E**), M2-macrophages (**G**) in presence or not of 25% (v:v) of HE SN and/or anti-PD-1. Results are expressed as the mean of intensity of each donor (N=1). Each condition was analysed in triplicate. Graphs were obtained with GraphPad Prism 8.4.3. Data are expressed as mean +/- SD, each point representing an independent test. Statistics were realised on the 50h data on GraphPad Prism 8.4.3. with a Shapiro-Wilk test to assess the normality and a one-way ANOVA, followed by a Tukey's multiple comparison test.

Abbreviations : CFSE, carboxyfluorescein succinimidyl ester; HE SN, human eosinophil supernatant; PD, programmed death cell.

PART IV

DISCUSSION

IV. DISCUSSION

Macrophages are highly versatile mononuclear cells of the innate immune system[22,31] and can fulfil various functions in tissues, including phagocytosis, antigen presentation and cytokines production[22,32,35]. Depending on environmental stimuli, macrophages can display different phenotypes[22,32]. Although incomplete[82], the M1/M2 polarisation models have been widely used to characterise the pro- and anti-inflammatory macrophages[12,22,36,40]. In cancer, tumour-associated macrophages mostly present the M2-phenotype and pro-tumoral properties[35,42], while, in MPM, high TAM infiltration correlates with worst OS[45,46].

On the other hand, eosinophils are highly pleiotropic immune cells[47] and contain granules[31] filled with cytotoxic proteins (*i.e.*, CLC-protein, ECP, EPO, MBP and EDN)[48,54,58]. Eosinophils arise from $CD34^+$ bone marrow HSC and mature through IL-5 stimulation[48,53,54]. Main function englobes degranulation, *i.e.*, discharge of cytoplasmic granules content and regulation of inflammation[48]. Eosinophils are recruited in the TME in response to different kinds of stimuli and can exert anti- or pro-tumoral roles[53].

In MPM, recent studies from the CME laboratory has demonstrated a negative impact of eosinophils on OS during chemotherapy treatment[50]. Besides, FDA has newly approved immunotherapeutic treatment involving the combination of nivolumab and ipilimumab, respectively anti-PD-1 and -CTLA-4 immune checkpoint inhibitors[25,27]. Therefore, this master thesis aimed to initiate the research on how eosinophils shape macrophages response to immunotherapy in MPM.

To do so, human primary macrophages were isolated, differentiated and polarised into the M1- and M2-phenotypes. The objective of this work was to assess (i) the phenotype of macrophages (ii) the effect of HE SN on PD-1 and PD-L1 expression and (iii) the cytotoxicity of macrophages towards MPM cells in presence of anti-PD-1 and HE SN.

12. Primary macrophages culture

Similar protocol (**Figure 9A**) for human primary macrophages culture has been widely used for decades and can be easily found in the literature. However, slight modifications can be observed from one article to another, especially regarding the cytokines concentration. Indeed, M-CSF can be used with a concentration between 10 and 100 ng/mL, LPS between 10 and 500 ng/mL, IFN-γ between 20 and 50 ng/mL and IL-4 between 10 and 20 ng/mL, while the concentration used were 100, 500, 20 and 20 ng/mL, respectively. Those concentrations changes may influence the polarisation and its intensity. Moreover, polarisation time can vary from 24 hours to 4 days and several other cytokines can be added during the process.[83–87] Indeed, GM-CSF is sometimes used for differentiation[83–86], while IL-10[83,86,87], involved in wound healing and inflammation resolution[84], and dexamethason[86] can be added to induce M2-polarization. However, GM-CSF tends to polarise macrophages into a M1-like

phenotype, while M-CSF can induce macrophages differentiation close from the M2-phenotype[22,32,83–86], even if polarisation into M1-phenotype after an M-CSF-induced differentiation remains possible[85].

Regarding macrophages morphology, research with a similar protocol shows corresponding data. Indeed, monocytes cytoplasmic volume increase during differentiation (**Figure 9B-C)**, leading to an increase in size[88], while specific spindle- and round-shape have been observed in the M1- (**Figure 9E**) and M2-phenotypes (**Figure 9F**), respectively[86,89,90].

13. Membrane receptors characterisation

13.1. Gating strategy for macrophages

Three different arguments support the presumption that the smaller population on FSC/SSC profiles is composed of death macrophages. Firstly, the PI dye intercalates in the DNA of compromised-membrane cells and has been used as a mortality dye by other scientists on primary macrophages and monocyte cell line (THP-1)[76,91–94]. Secondly, Zombie Aqua dye has also been used by numerous scientists on several macrophage types, including PBMCs-macrophages[95], alveolar macrophages[96], microglia (macrophages from central nerve system)[97], Kupffer cells (resident-liver macrophages)[98] and primary human macrophages[99]. Thirdly, since the process of cell apoptosis goes along with shrinkage[100,101], the smaller population (with lower FSC values) may be death.

Nevertheless, affirming with certainty that the smaller population encompasses death cells, while the larger population are living cells remains impossible for the following reasons. Firstly, PI can intercalate into all double-stranded nucleus acid, including double-stranded RNA as well. In this way, Rieger and al. found wrongly stained PI^+ cells in a sizeable proportion, especially in primary cells[77]. Secondly, as previously mentioned, macrophages main functions involve the phagocytosis[22,39]. Thereby, the hypothesis that living cells can phagocytose the dyes cannot be undoubtedly excluded. This mechanism has been investigated with AnnexinV dye because living macrophages phagocytose $AnnexinV^+$ apoptotic bodies and become positive as well[102].

Anyhow, the two macrophages populations on FSC/SSC profiles have been observed in similar articles[103,104] and the same gating strategy has been adopted by the authors. Hence, having a dead-cell population might be common.

13.2. Expression of membrane-associated receptors

As visible on **Figure 11B-C**, M1-macrophages overexpress CD80 and PD-L1, while the M2-phenotype express CD86, HLA-DR and highly CD206. Unstimulated macrophages only express HLA-DR. Moreover, PD-1 is hardly expressed. Additionally, some results present elevated variability. Although primary models based on peripherical blood immune cells are

more relevant than cell lines, human donors present larger variations between each other[105,106].

CD80 (also known as B7-1) works in tandem with CD86 in the activation of T-cells[18,107,108] and is well-known as a M1-phenotype marker[37,85,109]. Indeed, the M1-phenotype overexpresses this surface receptor[37,85,110], as found on the flow cytometry experiments presented. Moreover, IFN-γ stimulation enhances CD80[108], which correlates with M1-macrophages that are stimulated with this cytokines, while IL-10, an interleukin highly expressed by the M2-phenotype[33,35,37], downregulate CD80 expression[111]. Hence, by expressing IL-10, M2-macrophages could inhibit their own CD80 expression.

Besides, **CD86** (also known as B7-2) is the other co-stimulatory receptor responsible for T-cell activation[90,107,108] and, hence, is also a M1-phenotype marker[37,103,107,109]. In **Figure 11C**, CD86 has been shown to be expressed, not by the M1-, but by the M2-macrophages. The M1-phenotype not expressing CD86 is a questioning result as its expression is enhanced by IFN- γ stimualtion[108]. The presence of anergized macrophages might be an interesting hypothesis. If accepted, the non-expression of CD86 by M1-macrophages may lead to a decrease in T-cell activation properties. Aside, a M2-subtype, can also express CD86[107]. Termed M2b or regulatory macrophages, this subtype is induced by a combined exposure of immune complexes (IC) and Toll-like receptors (TLR) agonists and, in cancer, downregulate the immune system and enhance tumour development[22,107].

HLA-DR is part of the MHC class II molecules[79] and represent a good marker for both M1- and M2-phenotypes[112]. In the flow cytometry experiment (**Figure 11C**), results show that it is highly expressed by M0- and M2-macrophages. However, as a molecule involved in antigen presentation[79], HLA-DR expression is supposed to be enhanced by IFN-γ[108], which contrasts with obtained-results. Meanwhile, M2b can express HLA-DR[107]. To explain the expression by the M0-phenotype, the role of M-CSF in HLA-DR expression must be considered. As we already know, M-CSF drives macrophages polarisation towards a M2-phenotype[22,32,83–86].

CD206, the mannose receptor, is involved the recognition mannan from pathogen cell surface[40] and is typically a M2-phenotype marker[37,107,113]. In the flow cytometry experiment, CD206 is highly expressed by M2-macrophages, unlike the M0- and M1-phenotypes. This correlates with a similar experiment, which demonstrated that macrophages stimulated with IL-4 shown a boosted CD206 expression[108].

PD-1 is an immune checkpoint involved in T-cell activation and macrophages phagocytosis[12,29]. Results in **Figure 11C** show minor PD-1 expression and no difference between macrophages phenotype, even if a similar article shown an increased expression by M2-, compared to M1-macrophages[114].

PD-L1 is PD-1 ligand and is expressed by cancerous[19,30] and immune cells, including macrophages[12,108,111]. In **Figure 11B-C**, PD-L1 was expressed by M1- and, in a lesser extent, M2-macropages. These statements correlate with similar articles demonstrating that IFN-γ

stimulation highly increases PD-L1 expression[108,111], as well as IL-4 stimulation in a lesser extent[108]. Moreover, M2b-macrophages has also been found to express PD-L1[107].

Lastly, this experiment aimed to confirm the macrophages polarisation and potentially explains further results. In practice, results allow the formulation of hypothesis regarding macrophages phenotype. Indeed, with high CD86 and HLA-DR expression supplementing the well-established CD206 one, M2-macrophages can be considered as M2b-phenotype, a M2-subtype known as regulatory macrophages. Regarding the M1-phenotype, the absence of CD86 and HLA-DR expression is concerning and could be a consequence of the anergization of macrophages. Several possible explanations can be formulated. First, the polarisation time may be too long or the cytokines (IFN-γ and LPS) may be too concentrated, leading arguably in both cases to dying macrophages, as the M1-phenotype is known to succumb to its own NO production[22]. Besides, floating death cells in the culture may influence M1-macrophages during the polarisation, as macrophages can phagocytose particles, including dead cells. Finally, differentiation with M-CSF, which has been reported to be a M2-phenotype inducer[22,32,83–86], may also impact M1-polarization, even if the shift from M2- to M1-phenotype can occur in pro)inflammatory conditions[22,32]. Anyhow, the cytotoxic capacities of produced M1-macrophages may be questioned in following experiments.

13.3. Modulation of PD-1 and PD-L1 expression by eosinophils

13.3.1. Macrophages

HE SN appears to slightly diminish **PD-1** and **PD-L1** expression by macrophages (**Figure 12C-D**, non-significant). However, no similar experiment has been conducted on the impact on eosinophil cytokines on PD-1/PD-L1 pathways in macrophages. Further experiments should be carried out to determine the exact mechanisms and molecules involved in the inhibition of PD-1/PD-L1 pathways by eosinophils. To do so, HE SN cytokines content must be characterised. Several methods can be chosen, including chromatography, mass spectrometry, enzyme-linked immunosorbent assay (ELISA) and Multiplex immunoassay. Afterwards, highly produced molecules should be added in a macrophage culture for 48 hours before assessing the PD-1/PD-L1 expression.

13.3.2. MPM cells

Figure 13C-D shows that **PD-L1** and, in a lesser extent, **PD-1** are expressed by MPM cell lines, *i.e.*, M14K with epithelioid subtypes and ZL34 with sarcomatoid one[75]. ZL34 expression is slightly superior than M14K one. Similar articles show comparable results. In MPM, PD-1 was found in 10% of patients[115], while PD-L1 is expressed both in MPM cell lines[116] and *in vivo* tumour[117]. Moreover, sarcomatoid subtypes express PD-L1 in higher rates and with an augmented intensity[118].

Moreover, the modulation of PD-1 and PD-L1 expression by eosinophils on MPM cells (**Figure 13C-D**) was assessed and no significant variations could be demonstrated. Nevertheless, HE SN tends to diminish PD-L1 expression. Unfortunately, similar experiments were never conducted for MPM. Solely, Driscoll and al. (2017) demonstrated that eosinophils upregulate PD-L1 expression in multiple myeloma, which enhance immunosuppressive microenvironment[119]. Moreover, human eosinophil express PD-L1[120] and could therefore bind to PD-1 and exert the same pro-tumoral function as cancerous cells, namely reducing T-cell activation and macrophage phagocytosis properties.

As discussed above for macrophages (cf. 13.3.1. Macrophages), it might be interesting to point out the exact mechanisms and eosinophil-produced molecules that could influence PD-1 and PD-L1 expression by MPM cells.

14. Mortality assessment in MPM-macrophages co-culture

14.1. Cytotoxicity of primary macrophages towards MPM cells

The only significant difference in the cytotoxicity experiment has been found for the M14K cell lines, cultured with M0-macrophages (1:1) and supplemented with anti-PD-1 and HE SN, compared to the mock (no anti-PD-1 and no HE SN) (**Figure 16C**). Indeed, anti-PD-1, by inhibiting the PD-1/PD-L1 liaison, may repeal the immunosuppressive effect of HE SN.

Regarding macrophages phenotypes, although the M0-phenotype was closely related to the M2-phenotype before the co-culture (cf. 13.2. Expression of membrane-associated receptors), MPM co-cultured with M0-macrophages display a higher mortality rate than in M2-phenotype co-culture. Therefore, the polarisation switch of the M0-phenotype from the M2- to the M1-phenotype could be hypothesised. Besides, M1-macrophages do not exert a significant influence on MPM cells mortality. As explained above (cf. 13.2. Expression of membrane-associated receptors), M1-macrophages might be anergized and, hence, do not exert their anti-tumoral function. Finally, in M2-macrophages wells, MPM cells display the lowest mortality rates among co-cultures. Indeed, the M2-phenotype may be a regulatory phenotype, called M2b, and would therefore exhibit pro-tumoral properties.

Anyhow, regarding the low number of repetitions (two for ZL34 and one for M14K), further experiments are ongoing to validate the conclusions on macrophage cytotoxicity. A total of 10 repetitions were initially planned but, due to mortality problems and a lack of time, only a few have been conducted. Therefore, further studies with an acceptable number of repetitions must be carried out to properly study how eosinophils shape macrophages cytotoxicity towards MPM cells in an immunotherapeutic context.

PART V

CONCLUSION

V. CONCLUSION

To conclude, this master thesis contributes to highlight the influence of the eosinophil supernatant on the PD-1/PD-L1 pathways in macrophages and MPM cells, especially in the M1-phenotype. Further experiments should be conducted to discover which cytokine is involved. Secondly, it underlines the presence of a dead population in the flow cytometry experiments with PI and Zombie dyes. Moreover, the expression of CD80, CD86, HLA-DR, CD206, PD-1 and PD-L1 has been characterised in macrophages after M1- and M2-polarisation and the presence of anergized M1-macrophages and M2b phenotype has been hypothesised. Finally, this work initiates the research on how eosinophil supernatant shape macrophages response to immunotherapy in MPM.

VI. PERSONAL CONTRIBUTION

This master's thesis enabled me to investigate a field I was not initially familiar with. I had the opportunity to learn more about immunity and cancer research through the literature and to master the technique of primary macrophage isolation and culture, with the advice of M. Hamaïdia. The autonomy I had during the laboratories allowed me to acquire experiences on my manipulations. Throughout the project, I was supervised by my promoters, Louise Halkin and Luc Willems. They guided me to design my protocols and analyse the results.

PART VII

BIBLIOGRAPHY

VII. BIBLIOGRAPHY

[1] A. Scherpereel, G. Zalcman, and J. Margery, “Mésothéliome pleural malin,” Rev. Mal. Respir. Actual. **1**, S22–S26 (2009).

[2] S.E. Chen, and M.B. Pace, “Malignant pleural mesothelioma,” Am. J. Health. Syst. Pharm. **69**(5), 377–385 (2012).

[3] O. Melaiu, F. Gemignani, and S. Landi, “The genetic susceptibility in the development of malignant pleural mesothelioma,” J. Thorac. Dis. **10**(Suppl 2), S246–S252 (2018).

[4] A.L. Frank, and T.K. Joshi, “The Global Spread of Asbestos,” Ann. Glob. Health **80**(4), 257–262 (2014).

[5] R.-T. Lin, K. Takahashi, A. Karjalainen, T. Hoshuyama, D. Wilson, T. Kameda, C.-C. Chan, C.-P. Wen, S. Furuya, T. Higashi, L.-C. Chien, and M. Ohtaki, “Ecological association between asbestos-related diseases and historical asbestos consumption: an international analysis,” The Lancet **369**(9564), 844–849 (2007).

[6]“Amiante: danger de mort !,” SPF Santé Publique, (2016).

[7] A. Mansur, A.L. Potter, A.J. Zurovec, K.V. Nathamuni, R.R. Meyerhoff, M.F. Berry, A. Kang, and C.-F. Jeffrey Yang, “An Investigation of Cancer-Directed Surgery for Different Histologic Subtypes of Malignant Pleural Mesothelioma,” Chest **163**(5), 1292–1303 (2023).

[8] T.A. Yap, J.G. Aerts, S. Popat, and D.A. Fennell, “Novel insights into mesothelioma biology and implications for therapy,” Nat. Rev. Cancer **17**(8), 475–488 (2017).

[9] J.M. Seely, E.T. Nguyen, A.M. Churg, and N.L. Müller, “Malignant pleural mesothelioma: Computed tomography and correlation with histology,” Eur. J. Radiol. **70**(3), 485–491 (2009).

[10] G. Alì, R. Bruno, and G. Fontanini, “The pathological and molecular diagnosis of malignant pleural mesothelioma: a literature review,” J. Thorac. Dis. **10**(Suppl 2), S276–S284 (2018).

[11] L. Brcic, and I. Kern, “Clinical significance of histologic subtyping of malignant pleural mesothelioma,” Transl. Lung Cancer Res. **9**(3), 924–933 (2020).

[12] A.-L. Désage, G. Karpathiou, M. Peoc’h, and M.E. Froudarakis, “The Immune Microenvironment of Malignant Pleural Mesothelioma: A Literature Review,” Cancers **13**(13), 3205 (2021).

[13] I. Fiorilla, S. Martinotti, A.M. Todesco, G. Bonsignore, M. Cavaletto, M. Patrone, E. Ranzato, and V. Audrito, “Chronic Inflammation, Oxidative Stress and Metabolic Plasticity: Three Players Driving the Pro-Tumorigenic Microenvironment in Malignant Mesothelioma,” Cells **12**(16), 2048 (2023).

[14] H. Brossel, A. Fontaine, C. Hoyos, M. Jamakhani, M. Willems, M. Hamaidia, and L. Willems, “Activation of DNA Damage Tolerance Pathways May Improve Immunotherapy of Mesothelioma,” Cancers **13**(13), 3211 (2021).

[15] S. Toyokuni, “Iron addiction with ferroptosis-resistance in asbestos-induced mesothelial carcinogenesis: Toward the era of mesothelioma prevention,” Free Radic. Biol. Med. **133**, 206–215 (2019).

[16] G. Gaudino, J. Xue, and H. Yang, “How asbestos and other fibers cause mesothelioma,” Transl. Lung Cancer Res. **9**(Suppl 1), S39–S46 (2020).

[17] A. Xu, L.-J. Wu, R.M. Santella, and T.K. Hei, “Role of Oxyradicals in Mutagenicity and DNA Damage Induced by Crocidolite Asbestos in Mammalian Cells1,” Cancer Res. **59**(23), 5922–5926 (1999).

[18] J. Tedesco, M. Jaradeh, and W.T. Vigneswaran, “Malignant Pleural Mesothelioma: Current Understanding of the Immune Microenvironment and Treatments of a Rare Disease,” Cancers **14**(18), 4415 (2022).

[19] F. Napoli, A. Listì, V. Zambelli, G. Witel, P. Bironzo, M. Papotti, M. Volante, G. Scagliotti, and L. Righi, “Pathological Characterization of Tumour Immune Microenvironment (TIME) in Malignant Pleural Mesothelioma,” Cancers **13**(11), 2564 (2021).

[20] X. Ma, D. Lembersky, E.S. Kim, T.C. Bruno, J.R. Testa, and H.U. Osmanbeyoglu, “Spatial landscape of malignant pleural and peritoneal mesothelioma tumor immune microenvironment,” 2023.09.06.556559 (2023).

[21] H. Ollila, M.I. Mäyränpää, L. Paavolainen, J. Paajanen, K. Välimäki, E. Sutinen, H. Wolff, J. Räsänen, O. Kallioniemi, M. Myllärniemi, I. Ilonen, and T. Pellinen, “Prognostic Role of Tumour Immune Microenvironment in Pleural Epithelioid Mesothelioma,” Front. Oncol. **12**, 870352 (2022).

[22] P. Italiani, and D. Boraschi, “From Monocytes to M1/M2 Macrophages: Phenotypical vs. Functional Differentiation,” Front. Immunol. **5**, 514 (2014).

[23] F. Geissmann, S. Gordon, D.A. Hume, A.M. Mowat, and G.J. Randolph, “Unravelling mononuclear phagocyte heterogeneity,” Nat. Rev. Immunol. **10**(6), 453–460 (2010).

[24] S.M. Janes, D. Alrifai, and D.A. Fennell, “Perspectives on the Treatment of Malignant Pleural Mesothelioma,” N. Engl. J. Med. **385**(13), 1207–1218 (2021).

[25] A. Davis, H. Ke, S. Kao, and N. Pavlakis, “An Update on Emerging Therapeutic Options for Malignant Pleural Mesothelioma,” Lung Cancer Targets Ther. **13**, 1–12 (2022).

[26] T. Ito, S. Nakamura, Y. Kadomatsu, H. Ueno, T. Kato, N. Ozeki, K. Fukumoto, and T.F. Chen-Yoshikawa, “Impact of Pleural Thickness on Occurrence of Postoperative Complications in Patients with Malignant Pleural Mesothelioma,” Ann. Surg. Oncol. **30**(3), 1574–1583 (2023).

[27] O. of the Commissioner, “FDA Approves Drug Combination for Treating Mesothelioma,” FDA, (2020).

[28] P. Baas, A. Scherpereel, A. Nowak, N. Fujimoto, S. Peters, A. Tsao, A. Mansfield, S. Popat, T. Jahan, S. Antonia, Y. Oulkhouir, Y. Bautista, R. Cornelissen, L. Greillier, F. Grossi, D.M. Kowalski, J. Rodriguez-Cid, P. Aanur, C. Baudelet, and G. Zalcman, “ID:2908 First-Line Nivolumab + Ipilimumab vs Chemotherapy in Unresectable Malignant Pleural Mesothelioma: CheckMate 743,” J. Thorac. Oncol. **15**(10), e42 (2020).

[29] A.P.R. Bally, J.W. Austin, and J.M. Boss, “Genetic and Epigenetic Regulation of PD-1 Expression,” J. Immunol. **196**(6), 2431–2437 (2016).

[30] M. Hamaidia, H. Gazon, C. Hoyos, G.B. Hoffmann, R. Louis, B. Duysinx, and L. Willems, “Inhibition of EZH2 methyltransferase decreases immunoediting of mesothelioma cells by autologous macrophages through a PD-1–dependent mechanism,” JCI Insight **4**(18), e128474 (n.d.).

[31] B.T. Edelson, in *Gene Cell. Immunother. Cancer*, edited by A. Ghobadi and J.F. DiPersio (Springer International Publishing, Cham, 2022), pp. 13–25.

[32] I.N. Shalova, S. Saha, and S.K. Biswas, in *Inflammation* (John Wiley & Sons, Ltd, 2017), pp. 217–252.

[33] D.G. DeNardo, and B. Ruffell, “Macrophages as regulators of tumour immunity and immunotherapy,” Nat. Rev. Immunol. **19**(6), 369–382 (2019).

[34] S. Epelman, K.J. Lavine, and G.J. Randolph, “Origin and Functions of Tissue Macrophages,” Immunity **41**(1), 21–35 (2014).

[35] J. Austermann, J. Roth, and K. Barczyk-Kahlert, “The Good and the Bad: Monocytes’ and Macrophages’ Diverse Functions in Inflammation,” Cells **11**(12), 1979 (2022).

[36] C.D. Mills, K. Kincaid, J.M. Alt, M.J. Heilman, and A.M. Hill, “M-1/M-2 Macrophages and the Th1/Th2 Paradigm1,” J. Immunol. **164**(12), 6166–6173 (2000).

[37] C. Yunna, H. Mengru, W. Lei, and C. Weidong, “Macrophage M1/M2 polarization,” Eur. J. Pharmacol. **877**, 173090 (2020).

[38] N. Germic, Z. Frangez, S. Yousefi, and H.-U. Simon, “Regulation of the innate immune system by autophagy: monocytes, macrophages, dendritic cells and antigen presentation,” Cell Death Differ. **26**(4), 715–727 (2019).

[39] F. Kotsias, I. Cebrian, and A. Alloatti, in *Int. Rev. Cell Mol. Biol.*, edited by C. Lhuillier and L. Galluzzi (Academic Press, 2019), pp. 69–121.

[40] A. Aderem, and D.M. Underhill, “Mechanisms of Phagocytosis in Macrophages,” Annu. Rev. Immunol. **17**(1), 593–623 (1999).

[41] N. Jain, J. Moeller, and V. Vogel, “Mechanobiology of Macrophages: How Physical Factors Coregulate Macrophage Plasticity and Phagocytosis,” Annu. Rev. Biomed. Eng. **21**(1), 267–297 (2019).

[42] Z. Duan, and Y. Luo, “Targeting macrophages in cancer immunotherapy,” Signal Transduct. Target. Ther. **6**(1), 1–21 (2021).

[43] I.A. Ishina, M.Y. Zakharova, I.N. Kurbatskaia, A.E. Mamedov, A.A. Belogurov, and A.G. Gabibov, “MHC Class II Presentation in Autoimmunity,” Cells **12**(2), 314 (2023).

[44] G. Arango Duque, and A. Descoteaux, “Macrophage Cytokines: Involvement in Immunity and Infectious Diseases,” Front. Immunol. **5**, 491 (2014).

[45] H. Ujiie, K. Kadota, J. Nitadori, J.G. Aerts, K.M. Woo, C.S. Sima, W.D. Travis, D.R. Jones, L.M. Krug, and P.S. Adusumilli, “The tumoral and stromal immune microenvironment in malignant pleural mesothelioma: A comprehensive analysis reveals prognostic immune markers,” OncoImmunology **4**(6), e1009285 (2015).

[46] B.M. Burt, S.J. Rodig, T.R. Tilleman, A.W. Elbardissi, R. Bueno, and D.J. Sugarbaker, “Circulating and tumor-infiltrating myeloid cells predict survival in human pleural mesothelioma,” Cancer **117**(22), 5234–5244 (2011).

[47] T. Marichal, C. Mesnil, and F. Bureau, “Homeostatic Eosinophils: Characteristics and Functions,” Front. Med. **4**, (2017).

[48] H.F. Rosenberg, “Eosinophils,” Encycl. Immunobiol., 334–344 (2016).

[49] T. Fettrelet, L. Gigon, A. Karaulov, S. Yousefi, and H.-U. Simon, “The Enigma of Eosinophil Degranulation,” Int. J. Mol. Sci. **22**(13), 7091 (2021).

[50] M. Willems, A. Scherpereel, E. Wasielewski, J. Raskin, H. Brossel, A. Fontaine, M. Grégoire, L. Halkin, M. Jamakhani, V. Heinen, R. Louis, B. Duysinx, M. Hamaidia, and L. Willems, “Excess of blood

eosinophils prior to therapy correlates with worse prognosis in mesothelioma," Front. Immunol. **14**, 148798 (2023).

[51] P. Valent, A.D. Klion, F. Roufosse, D. Simon, G. Metzgeroth, K.M. Leiferman, J. Schwaab, J.H. Butterfield, W.R. Sperr, K. Sotlar, P. Vandenberghe, G. Hoermann, T. Haferlach, R. Moriggl, T.I. George, C. Akin, B.S. Bochner, J. Gotlib, A. Reiter, H.-P. Horny, M. Arock, H.-U. Simon, and G.J. Gleich, "Proposed refined diagnostic criteria and classification of eosinophil disorders and related syndromes," Allergy **78**(1), 47–59 (2023).

[52] A. Matucci, F. Nencini, G. Maggiore, F. Chiccoli, M. Accinno, E. Vivarelli, C. Bruno, L.G. Locatello, A. Palomba, E. Nucci, V. Mecheri, M. Perlato, O. Rossi, P. Parronchi, E. Maggi, O. Gallo, and A. Vultaggio, "High proportion of inflammatory CD62Llow eosinophils in blood and nasal polyps of severe asthma patients," Clin. Exp. Allergy **53**(1), 78–87 (2023).

[53] S. Grisaru-Tal, M. Itan, A.D. Klion, and A. Munitz, "A new dawn for eosinophils in the tumour microenvironment," Nat. Rev. Cancer **20**(10), 594–607 (2020).

[54] C. Blanchard, and M.E. Rothenberg, in *Adv. Immunol.* (Academic Press, 2009), pp. 81–121.

[55] S.E.W. Jacobsen, and C. Nerlov, "Haematopoiesis in the era of advanced single-cell technologies," Nat. Cell Biol. **21**(1), 2–8 (2019).

[56] X. Xie, M. Liu, Y. Zhang, B. Wang, C. Zhu, C. Wang, Q. Li, Y. Huo, J. Guo, C. Xu, L. Hu, A. Pang, S. Ma, L. Wang, W. Cao, S. Chen, Q. Li, S. Zhang, X. Zhao, W. Zhou, H. Luo, G. Zheng, E. Jiang, S. Feng, L. Chen, L. Shi, H. Cheng, S. Hao, P. Zhu, and T. Cheng, "Single-cell transcriptomic landscape of human blood cells," Natl. Sci. Rev. **8**(3), nwaa180 (2021).

[57] C. Nerlov, K.M. McNagny, G. Döderlein, E. Kowenz-Leutz, and T. Graf, "Distinct C/EBP functions are required for eosinophil lineage commitment and maturation," Genes Dev. **12**(15), 2413–2423 (1998).

[58] K.R. Acharya, and S.J. Ackerman, "Eosinophil Granule Proteins: Form and Function," J. Biol. Chem. **289**(25), 17406–17415 (2014).

[59] M.M. Grozdanovic, C.B. Doyle, L. Liu, B.T. Maybruck, M.A. Kwatia, N. Thiyagarajan, K.R. Acharya, and S.J. Ackerman, "Charcot-Leyden crystal protein/galectin-10 interacts with cationic ribonucleases and is required for eosinophil granulogenesis," J. Allergy Clin. Immunol. **146**(2), 377-389.e10 (2020).

[60] M.E. Rothenberg, and S.P. Hogan, "The Eosinophil," Annu. Rev. Immunol. **24**(1), 147–174 (2006).

[61] P. Ilmarinen, E. Moilanen, and H. Kankaanranta, "Regulation of Spontaneous Eosinophil Apoptosis—A Neglected Area of Importance," J. Cell Death **7**, JCD.S13588 (2014).

[62] G.M. Walsh, "Eosinophil Apoptosis and Clearance in Asthma," J. Cell Death **6**, JCD.S10818 (2013).

[63] H. Reichman, D. Karo-Atar, and A. Munitz, "Emerging Roles for Eosinophils in the Tumour Microenvironment," Trends Cancer **2**(11), 664–675 (2016).

[64] G. Varricchi, M.R. Galdiero, S. Loffredo, V. Lucarini, G. Marone, F. Mattei, G. Marone, and G. Schiavoni, "Eosinophils: The unsung heroes in cancer?," OncoImmunology **7**(2), e1393134 (2018).

[65] J.M. da Silva, T.P. Moreira dos Santos, L.M. Sobral, C.M. Queiroz-Junior, M.A. Rachid, A.E.I. Proudfoot, G.P. Garlet, A.C. Batista, M.M. Teixeira, A.M. Leopoldino, R.C. Russo, and T.A. Silva, "Relevance of CCL3/CCR5 axis in oral carcinogenesis," Oncotarget **8**(31), 51024–51036 (2017).

[66] A. Yasukawa, K. Hosoki, M. Toda, Y. Miyake, Y. Matsushima, T. Matsumoto, D. Boveda-Ruiz, P. Gil-Bernabe, M. Nagao, M. Sugimoto, Y. Hiraguchi, R. Tokuda, M. Naito, T. Takagi, C.N. D'Alessandro-Gabazza, S. Suga, T. Kobayashi, T. Fujisawa, O. Taguchi, and E.C. Gabazza, "Eosinophils Promote Epithelial to Mesenchymal Transition of Bronchial Epithelial Cells," PLOS ONE **8**(5), e64281 (2013).

[67] R. Zaynagetdinov, T.P. Sherrill, L.A. Gleaves, A.G. McLoed, J.A. Saxon, A.C. Habermann, L. Connelly, D. Dulek, R.S. Peebles Jr., B. Fingleton, F.E. Yull, G.T. Stathopoulos, and T.S. Blackwell, "Interleukin-5 Facilitates Lung Metastasis by Modulating the Immune Microenvironment," Cancer Res. **75**(8), 1624–1634 (2015).

[68] B. Zhang, C.-Y. Wei, K.-K. Chang, J.-J. Yu, W.-J. Zhou, H.-L. Yang, J. Shao, J.-J. Yu, M.-Q. Li, and F. Xie, "TSLP promotes angiogenesis of human umbilical vein endothelial cells by strengthening the crosstalk between cervical cancer cells and eosinophils," Oncol. Lett. **14**(6), 7483–7488 (2017).

[69] S.O. Odemuyiwa, A. Ghahary, Y. Li, L. Puttagunta, J.E. Lee, S. Musat-Marcu, A. Ghahary, and R. Moqbel, "Cutting Edge: Human Eosinophils Regulate T Cell Subset Selection through Indoleamine 2,3-Dioxygenase1," J. Immunol. **173**(10), 5909–5913 (2004).

[70] P.M. Furbert-Harris, D. Parish-Gause, K.A. Hunter, T.R. Vaughn, C. Howland, J. Okomo-Awich, K. Forrest, I. Laniyan, A. Abdelnaby, and O.A. Oredipe, "Activated eosinophils upregulate the metastasis suppressor molecule E-cadherin on prostate tumor cells," Cell. Mol. Biol. Noisy--Gd. Fr. **49**(7), 1009–1016 (2003).

[71] V. Lucarini, G. Ziccheddu, I. Macchia, V. La Sorsa, F. Peschiaroli, C. Buccione, A. Sistigu, M. Sanchez, S. Andreone, M.T. D'Urso, M. Spada, D. Macchia, C. Afferni, F. Mattei, and G. Schiavoni, "IL-33 restricts tumor growth and inhibits pulmonary metastasis in melanoma-bearing mice through eosinophils," OncoImmunology **6**(6), e1317420 (2017).

[72] L. Simson, J.I. Ellyard, L.A. Dent, K.I. Matthaei, M.E. Rothenberg, P.S. Foster, M.J. Smyth, and C.R. Parish, "Regulation of Carcinogenesis by IL-5 and CCL11: A Potential Role for Eosinophils in Tumour Immune Surveillance1," J. Immunol. **178**(7), 4222–4229 (2007).

[73] S. Kataoka, Y. Konishi, Y. Nishio, K. Fujikawa-Adachi, and A. Tominaga, "Antitumor Activity of Eosinophils Activated by IL-5 and Eotaxin against Hepatocellular Carcinoma," DNA Cell Biol. **23**(9), 549–560 (2004).

[74] G.T. Stathopoulos, T.P. Sherrill, S.P. Karabela, K. Goleniewska, I. Kalomenidis, C. Roussos, B. Fingleton, F.E. Yull, R.S. Peebles, and T.S. Blackwell, "Host-derived interleukin-5 promotes adenocarcinoma-induced malignant pleural effusion," Am. J. Respir. Crit. Care Med. **182**(10), 1273–1281 (2010).

[75] R.M. Jagirdar, E. Apostolidou, P.A. Molyvdas, K.I. Gourgoulianis, C. Hatzoglou, and S.G. Zarogiannis, "Influence of AQP1 on cell adhesion, migration, and tumor sphere formation in malignant pleural mesothelioma is substratum- and histological-type dependent," Am. J. Physiol.-Lung Cell. Mol. Physiol. **310**(6), L489–L495 (2016).

[76] N. Pick, S. Cameron, D. Arad, and Y. Av-Gay, "Screening of Compounds Toxicity against Human Monocytic cell line-THP-1 by Flow Cytometry," Biol. Proced. Online **6**, 220–225 (2004).

[77] A.M. Rieger, B.E. Hall, L.T. Luong, L.M. Schang, and D.R. Barreda, "Conventional apoptosis assays using propidium iodide generate a significant number of false positives that prevent accurate assessment of cell death," J. Immunol. Methods **358**(1), 81–92 (2010).

[78]"Live Cell/Dead Cell Discrimination," (n.d.).

[79] M.R. Dunne, J.J. Phelan, A.J. Michielsen, A.A. Maguire, C. Dunne, P. Martin, S. Noonan, M. Tosetto, R. Geraghty, D. Fennelly, K. Sheahan, E.J. Ryan, and J. O'Sullivan, "Characterising the prognostic potential of HLA-DR during colorectal cancer development," Cancer Immunol. Immunother. **69**(8), 1577–1588 (2020).

[80] H. Cai, Y. Zhang, J. Wang, and J. Gu, "Defects in Macrophage Reprogramming in Cancer Therapy: The Negative Impact of PD-L1/PD-1," Front. Immunol. **12**, 690869 (2021).

[81] J. Savill, V. Fadok, P. Henson, and C. Haslett, "Phagocyte recognition of cells undergoing apoptosis," Immunol. Today **14**(3), 131–136 (1993).

[82] D.M. Mosser, and J.P. Edwards, "Exploring the full spectrum of macrophage activation," Nat. Rev. Immunol. **8**(12), 958–969 (2008).

[83] A. Kelly, A.M. Grabiec, and M.A. Travis, in *Macrophages Methods Protoc.*, edited by G. Rousselet (Springer, New York, NY, 2018), pp. 1–11.

[84] F.J. Rios, R.M. Touyz, and A.C. Montezano, in *Hypertens. Methods Protoc.*, edited by R.M. Touyz and E.L. Schiffrin (Springer, New York, NY, 2017), pp. 311–320.

[85] M. Jaguin, N. Houlbert, O. Fardel, and V. Lecureur, "Polarization profiles of human M-CSF-generated macrophages and comparison of M1-markers in classically activated macrophages from GM-CSF and M-CSF origin," Cell. Immunol. **281**(1), 51–61 (2013).

[86] D.Y.S. Vogel, J.E. Glim, A.W.D. Stavenuiter, M. Breur, P. Heijnen, S. Amor, C.D. Dijkstra, and R.H.J. Beelen, "Human macrophage polarization in vitro: Maturation and activation methods compared," Immunobiology **219**(9), 695–703 (2014).

[87] C. Clavel, L. Ceccato, F. Anquetil, G. Serre, and M. Sebbag, "Among human macrophages polarised to different phenotypes, the M-CSF-oriented cells present the highest pro-inflammatory response to the rheumatoid arthritis-specific immune complexes containing ACPA," Ann. Rheum. Dis. **75**(12), 2184–2191 (2016).

[88] S. Eligini, M. Crisci, E. Bono, P. Songia, E. Tremoli, G.I. Colombo, and S. Colli, "Human monocyte-derived macrophages spontaneously differentiated in vitro show distinct phenotypes," J. Cell. Physiol. **228**(7), 1464–1472 (2013).

[89] F. Porcheray, S. Viaud, A.-C. Rimaniol, C. Léone, B. Samah, N. Dereuddre-Bosquet, D. Dormont, and G. Gras, "Macrophage activation switching: an asset for the resolution of inflammation," Clin. Exp. Immunol. **142**(3), 481–489 (2005).

[90] S. Tedesco, C. Bolego, A. Toniolo, A. Nassi, G.P. Fadini, M. Locati, and A. Cignarella, "Phenotypic activation and pharmacological outcomes of spontaneously differentiated human monocyte-derived macrophages," Immunobiology **220**(5), 545–554 (2015).

[91] I. Catelas, O.L. Huk, A. Petit, D.J. Zukor, R. Marchand, and L. Yahia, "Flow cytometric analysis of macrophage response to ceramic and polyethylene particles: Effects of size, concentration, and composition," J. Biomed. Mater. Res. **41**(4), 600–607 (1998).

[92] I. Catelas, A. Petit, D.J. Zukor, J. Antoniou, and O.L. Huk, "TNF-α secretion and macrophage mortality induced by cobalt and chromium ions in vitro-Qualitative analysis of apoptosis," Biomaterials **24**(3), 383–391 (2003).

[93] K.-W. Wong, and W.R. Jacobs Jr, "Mycobacteriumtuberculosis Exploits Human Interferon γ to Stimulate Macrophage Extracellular Trap Formation and Necrosis," J. Infect. Dis. **208**(1), 109–119 (2013).

[94] S.-L. Tran, E. Guillemet, M. Ngo-Camus, C. Clybouw, A. Puhar, A. Moris, M. Gohar, D. Lereclus, and N. Ramarao, "Haemolysin II is a Bacillus cereus virulence factor that induces apoptosis of macrophages," Cell. Microbiol. **13**(1), 92–108 (2011).

[95] M.W. Buchanan, B.D. Furman, J.H. Zeitlin, J.L. Huebner, V.B. Kraus, J.S. Yi, and S.A. Olson, "Degenerative joint changes following intra-articular fracture are more severe in mice with T cell deficiency," J. Orthop. Res. **39**(8), 1710–1721 (2021).

[96] P.J.R. Price, Z. Bánki, A. Scheideler, H. Stoiber, A. Verschoor, G. Sutter, and M.H. Lehmann, "Complement component C5 recruits neutrophils in the absence of C3 during respiratory infection with modified vaccinia virus Ankara," J. Immunol. Baltim. Md 1950 **194**(3), 1164–1168 (2015).

[97] L.M. Healy, M. Yaqubi, S. Ludwin, and J.P. Antel, "Species differences in immune-mediated CNS tissue injury and repair: A (neuro)inflammatory topic," Glia **68**(4), 811–829 (2020).

[98] S. Daemen, M.M. Chan, and J.D. Schilling, "Comprehensive analysis of liver macrophage composition by flow cytometry and immunofluorescence in murine NASH," STAR Protoc. **2**(2), 100511 (2021).

[99] S. Rueschenbaum, C. Cai, M. Schmidt, K. Schwarzkopf, U. Dittmer, S. Zeuzem, C. Welsch, and C.M. Lange, "Translation of IRF-1 Restricts Hepatic Interleukin-7 Production to Types I and II Interferons: Implications for Hepatic Immunity," Front. Immunol. **11**, 581352 (2021).

[100] Y. Wen, Z. Chen, J. Lu, E. Ables, J.-L. Scemama, L.V. Yang, J.Q. Lu, and X.-H. Hu, "Quantitative analysis and comparison of 3D morphology between viable and apoptotic MCF-7 breast cancer cells and characterization of nuclear fragmentation," PLOS ONE **12**(9), e0184726 (2017).

[101] C.M. Henry, E. Hollville, and S.J. Martin, "Measuring apoptosis by microscopy and flow cytometry," Methods **61**(2), 90–97 (2013).

[102] D. Wlodkowic, W. Telford, J. Skommer, and Z. Darzynkiewicz, "Apoptosis and Beyond: Cytometry in Studies of Programmed Cell Death," Methods Cell Biol. **103**, 55–98 (2011).

[103] R.K. Keswani, G.S. Yoon, S. Sud, K.A. Stringer, and G.R. Rosania, "A far-red fluorescent probe for flow cytometry and image-based functional studies of xenobiotic sequestering macrophages," Cytometry A **87**(9), 855–867 (2015).

[104] A.R. Gómez-López, G. Manich, M. Recasens, B. Almolda, B. González, and B. Castellano, "Evaluation of Myelin Phagocytosis by Microglia/Macrophages in Nervous Tissue Using Flow Cytometry," Curr. Protoc. **1**(3), e73 (2021).

[105] O. Sharif, V.N. Bolshakov, S. Raines, P. Newham, and N.D. Perkins, "Transcriptional profiling of the LPS induced NF-κB response in macrophages," BMC Immunol. **8**(1), 1 (2007).

[106] Y. Li, M. Oosting, P. Deelen, I. Ricaño-Ponce, S. Smeekens, M. Jaeger, V. Matzaraki, M.A. Swertz, R.J. Xavier, L. Franke, C. Wijmenga, L.A.B. Joosten, V. Kumar, and M.G. Netea, "Inter-individual variability and genetic influences on cytokine responses to bacteria and fungi," Nat. Med. **22**(8), 952–960 (2016).

[107] L. Wang, S. Zhang, H. Wu, X. Rong, and J. Guo, “M2b macrophage polarization and its roles in diseases,” J. Leukoc. Biol. **106**(2), 345–358 (2019).

[108] G.V. Suarez, C. del C. Melucci Ganzarain, M.B. Vecchione, C.A. Trifone, J.L. Marín Franco, M. Genoula, E.J. Moraña, L. Balboa, and M.F. Quiroga, “PD-1/PD-L1 Pathway Modulates Macrophage Susceptibility to Mycobacterium tuberculosis Specific CD8+ T cell Induced Death,” Sci. Rep. **9**(1), 187 (2019).

[109] S. Soldano, A.C. Trombetta, P. Contini, V. Tomatis, B. Ruaro, R. Brizzolara, P. Montagna, A. Sulli, S. Paolino, C. Pizzorni, V. Smith, and M. Cutolo, “Increase in circulating cells coexpressing M1 and M2 macrophage surface markers in patients with systemic sclerosis,” Ann. Rheum. Dis. **77**(12), 1842–1845 (2018).

[110] P. Wisitpongpun, P. Potup, and K. Usuwanthim, “Oleamide-Mediated Polarization of M1 Macrophages and IL-1β Production by Regulating NLRP3-Inflammasome Activation in Primary Human Monocyte-Derived Macrophages,” Front. Immunol. **13**, 856296 (2022).

[111] J. Zhou, S. Zhang, and C. Guo, “Crosstalk between macrophages and natural killer cells in the tumor microenvironment,” Int. Immunopharmacol. **101**, 108374 (2021).

[112] C.H. Jiang, W.H. Liang, F.P. Li, Y.F. Xie, X. Yuan, H.J. Zhang, M. Li, J.F. Li, A.Z. Zhang, L. Yang, C.X. Liu, L.J. Pang, F. Li, and J.M. Hu, “Distribution and prognostic impact of M1 macrophage on esophageal squamous cell carcinoma,” Carcinogenesis **42**(4), 537–545 (2021).

[113] S. Mia, A. Warnecke, X.-M. Zhang, V. Malmström, and R.A. Harris, “An optimized Protocol for Human M2 Macrophages using M-CSF and IL-4/IL-10/TGF-β Yields a Dominant Immunosuppressive Phenotype,” Scand. J. Immunol. **79**(5), 305–314 (2014).

[114] S.R. Gordon, R.L. Maute, B.W. Dulken, G. Hutter, B.M. George, M.N. McCracken, R. Gupta, J.M. Tsai, R. Sinha, D. Corey, A.M. Ring, A.J. Connolly, and I.L. Weissman, “PD-1 expression by tumour-associated macrophages inhibits phagocytosis and tumour immunity,” Nature **545**(7655), 495–499 (2017).

[115] E. Marcq, V. Siozopoulou, J. De Waele, J. van Audenaerde, K. Zwaenepoel, E. Santermans, N. Hens, P. Pauwels, J.P. van Meerbeeck, and E.L.J. Smits, “Prognostic and predictive aspects of the tumor immune microenvironment and immune checkpoints in malignant pleural mesothelioma,” OncoImmunology **6**(1), e1261241 (2017).

[116] A. Scherpereel, F. Wallyn, S.M. Albelda, and C. Munck, “Novel therapies for malignant pleural mesothelioma,” Lancet Oncol. **19**(3), e161–e172 (2018).

[117] A.S. Mansfield, A.C. Roden, T. Peikert, Y.M. Sheinin, S.M. Harrington, C.J. Krco, H. Dong, and E.D. Kwon, “B7-H1 Expression in Malignant Pleural Mesothelioma is Associated with Sarcomatoid Histology and Poor Prognosis,” J. Thorac. Oncol. **9**(7), 1036–1040 (2014).

[118] S. Muller, W. Victoria Lai, P.S. Adusumilli, P. Desmeules, D. Frosina, A. Jungbluth, A. Ni, T. Eguchi, W.D. Travis, M. Ladanyi, M.G. Zauderer, and J.L. Sauter, “V-domain Ig-containing suppressor of T-cell activation (VISTA), a potentially targetable immune checkpoint molecule, is highly expressed in epithelioid malignant pleural mesothelioma,” Mod. Pathol. **33**(2), 303–311 (2020).

[119] J. Driscoll, I. Aslam, and E. Malek, “Eosinophils Upregulate PD-L1 and PD-L2 Expression to Enhance the Immunosuppressive Microenvironment in Multiple Myeloma,” Blood **130**, 4417 (2017).

[120] S. Pesce, F.B. Thoren, C. Cantoni, C. Prato, L. Moretta, A. Moretta, and E. Marcenaro, “The Innate Immune Cross Talk between NK Cells and Eosinophils Is Regulated by the Interaction of Natural Cytotoxicity Receptors with Eosinophil Surface Ligands,” Front. Immunol. **8**, (2017).